Microscopic Description of the Inelastic Proton Decay of Analog Resonances*

S. A. A. ZAIDI AND P. DYER†
The University of Texas, Austin, Texas 78712
(Received 20 March 1969)

A microscopic description of analog resonances is presented in the framework of the shell-model theory. The separation of the total Hamiltonian into an independent-particle Hamiltonian H_0 and the residual interaction V is discussed. A choice of H_0 is made that minimizes the residual interaction—in particular, the matrix elements between the continuum eigenstates of H_0. The diagonalization of the two-body residual interaction on an appropriately chosen set of $2p$-$1h$ configurations is carried out, and the numerical results are presented for ^{209}Bi. A group of $\frac{9}{2}^+$ states of analog spin $W_<$ is predicted to be about 11 MeV below the $g_{9/2}$ analog resonance in ^{209} Bi. Coupling of the various continua to the $W_>$ state gives rise to the isobaric analog resonance in the corresponding channels. The inelastic proton decay of the $g_{9/2}$ analog resonance in ^{209}Bi to the particle-hole states of ^{208}Pb is calculated, and the results are compared with experimental data. An expression for the energy-average S-matrix elements is derived starting from the multilevel expression describing the coupling of both $T_>$ and $T_<$ states to the various continua. There expressions differ from those given by Weidenmüller and by Mekjian and MacDonald and are in agreement with Robson's results in the one-channel case. Our expressions also agree with recent results obtained by Tamura.

I. INTRODUCTION

THE study of isobaric analog resonances has provided us with a useful tool for the determination of nuclear structure of the parent analog states. From an analysis of the elastic scattering of protons through isobaric analog resonances, it is now possible to determine the neutron-spectroscopic factors of the low-lying states of nuclei with an accuracy comparable to or even better than that obtained using the (d, p) stripping reaction. The inelastic proton decay of the isobaric analog resonances, however, is capable of yielding very important nuclear-structure information. This was first realized by Allan,[1] and a large number of papers[2] since have been devoted to the study of inelastic proton decay of these resonances. There are two fairly distinct mechanisms involved, either of which can lead to the decay of an isobaric analog resonance into an inelastic proton channel. The first situation arises when the low-lying states of the parent-analog nucleus contain admixtures of the collective excited states of the target nucleus. In this case one expects the analog resonances to decay to the corresponding excited state of the target. This situation, originally studied by Allan,[1] has been observed[3–7] in a number of nuclei and analyzed in terms of the weak-coupling model.

In heavy nuclei, particularly in the lead region, the analog resonances occur at an excitation energy of the order of 20 MeV. These resonances decay into a large number of inelastic proton channels[3–12] populating the excited states of the target nucleus up to 6 MeV in excitation energy. The inelastic scattering of protons from ^{208}Pb proceeding through the isobaric analog resonances in ^{209}Bi is particularly interesting. In this case the analog resonances are caused by the isobaric analogs of the nearly pure single-particle states[13–15] of ^{209}Pb. The inelastic decay of these resonances populates states in ^{208}Pb, many of which are superpositions of simple particle-hole states. There is considerable experimental evidence in favor of this simple interpretation. The inelastic proton scattering leading to the 4^- state in ^{208}Pb has been analyzed by Bondorf *et al.*[16] In their analysis these authors employed single-particle decay widths deduced from the inelastic scattering of protons from ^{207}Pb. This ingenious technique has rather limited application and requires a significant correction of the partial widths, to take into account the difference in energy of the outgoing proton. Their

* Work supported in part by the U.S. Atomic Energy Commission.
† Present address: California Institute of Technology, Pasadena, Calif.
[1] D. L. Allan, Phys. Letters **14**, 311 (1965).
[2] G. M. Temmer, in *Isospin in Nuclear Physics*, edited by D. H. Wilkinson (North-Holland Publishing Co., Amsterdam, 1969).
[3] S. A. A. Zaidi, P. von Brentano, and J. P. Wurm, Phys. Letters **19**, 45 (1965).
[4] E. J. Schneid, E. W. Hamburger, and B. L. Cohen, Phys. Rev. **161**, 1208 (1967).
[5] C. F. Moore, J. J. Kent, and S. A. A. Zaidi, Phys. Rev. Letters **18**, 345 (1967).
[6] N. Stein, C. A. Whitten, Jr., and D. A. Bromley, Phys. Rev. Letters **20**, 113 (1968).
[7] K. P. Lieb, J. J. Kent, and C. F. Moore, Phys. Rev. **175**, 1482 (1968).
[8] C. D. Kavaloski, J. S. Lilley, P. Richard, and N. Stein, Phys. Rev. Letters **16**, 807 (1966).
[9] S. A. A. Zaidi, J. L. Parish, J. G. Kulleck, C. F. Moore, and P. von Brentano, Phys. Rev. **165**, 1312 (1968).
[10] C. F. Moore, J. G. Kulleck, P. von Brentano, and F. Rickey, Phys. Rev. **164**, 1559 (1967).
[11] G. H. Lenz and G. M. Temmer, Nucl. Phys. **A112**, 625 (1968).
[12] P. Richard, N. Stein, C. D. Kavaloski, and J. S. Lilley, Phys. Rev. **171**, 1308 (1968).
[13] G. Muehllehner, A. S. Poltorak, W. C. Parkinson, and R. H. Bassel, Phys. Rev. **159**, 1039 (1967).
[14] G. J. Igo, P. D. Barnes, E. R. Flynn, and D. D. Armstrong, Phys. Rev. **177**, 1831 (1969).
[15] S. A. A. Zaidi and S. Darmodjo, Phys. Rev. Letters **19**, 1446 (1967).
[16] J. P. Bondorf, P. von Brentano, and P. Richard, Phys. Letters **27B**, 5 (1968).

analysis, however, yielded a neutron–neutron-hole configuration for the 4^- state, in agreement with shell-model calculations.

In this paper we report a description of the isobaric analog resonances that is based directly on the shell-model theory of nuclear reactions.[17–20] The basic assumption underlying this description, which is common to all shell-model calculations, is that there exists a *small* set of eigenstates of the independent-particle Hamiltonian H_0, such that the diagonalization of the effective residual interaction V on this set yields wave functions that provide an adequate description of the physical situation under consideration. In the description of nuclear reactions initiated by a nucleon incident upon a target nucleus, it is necessary to consider eigenstates of H_0 with at least one nucleon in the continuum. The inclusion of configurations with more than one nucleon in the continuum is beset with difficulties. We shall ignore such configurations altogether. The set of functions on which the residual interaction is to be diagonalized includes, then, functions characterized by a continuous-energy variable corresponding to a nucleon in the continuum. It is, however, possible to choose a finite number of configurations of this type together with a finite number of entirely bound configurations.

The proper choice of the Hamiltonian H_0 is crucial to a successful application of the shell-model approach to nuclear reactions. The main reason for this lies in the necessity for diagonalization of the residual interaction on the set of configurations involving one nucleon in the continuum. This diagonalization constitutes one of the basic practical difficulties of the shell-model approach to reaction theory and in practice can at best be carried out in Born approximation. In view of the approximate treatment of the continuum-continuum interaction, it is important to choose H_0 and V very carefully, so that the terms that have to be treated approximately are small relative to the ones to be treated exactly. Such considerations suggest the inclusion in H_0 of all those components of the residual interaction, the inclusion of which will not interfere with the exact diagonalization of H_0 on the space of configurations chosen. More specifically, one should construct simple interactions, like an "effective one-body potential", subtract these from the residual interaction V, and then compensate by adding the same simple interaction to H_0. This is basically the approach adopted by MacDonald.[18] In choosing H_0, attention must be paid to the single-particle resonances displayed by the continuum solutions of H_0. The matrix elements of the continuum-continuum interaction are strongly enhanced in the vicinity of the single-particle resonances, and an approximate treatment of the continuum-continuum interaction employing the Born series becomes questionable. If, however, the single-particle resonances are "sufficiently sharp" (i.e., occur low enough in energy) they can be handled, roughly speaking, in much the same way bound eigenstates of H_0 are treated. Techniques for treating such single-particle resonances are discussed by Weidenmüller[19,20] and also by Garside and MacDonald.[21] It must be pointed out, however, that these techniques are useful *only* when the resonances are in fact sufficiently shap. Thus a second criterion for a good choice of H_0 is that the single-particle resonances occur at low enough energies so that techniques similar to those of the above references can be applied.

The theory of isobaric analog resonances given by Weidenmüller[22] is based on a choice of H_0 which is useful for an understanding of the nature of these resonances; however, the continuum eigenstates of H_0 display single-particle resonances very close to the energy of the isobaric analog resonance. These single-particle resonances are, in general, too broad for the techniques of Ref. 22 to apply. Weidenmüller gives arguments for factorizing the energy dependence of the continuum functions in the neighborhood of the single-particle resonances. The contributions from the single-particle resonances are then represented as a sum of separable terms, and the remaining part of the continuum-continuum interaction is deleted.

We choose an independent-particle Hamiltonian such that the only well-pronounced single-particle resonances displayed by its solution occur below the Coulomb barrier and have very small widths (typically less than 1 keV). Our choice of the independent-particle Hamiltonian corresponds to the inclusion in H_0 of a large component of the residual interaction which, in the phenomenological description, has its counterpart in the well-known symmetry term of the optical potential for nucleons. Clearly, the residual interaction is considerably reduced with this choice of H_0. The residual interaction is then diagonalized on a suitably chosen set of bound configurations and of configurations involving a single proton in the continuum. The continuum-continuum part of the residual interaction is neglected, but we expect that with our choice of H_0 this interaction is very weak in general. Exceptions might, however, arise in dealing with the collective states of the target nucleus.

The diagonalization of the residual interaction on the bound eigenstates of H_0 yields a state $|\Sigma\rangle$ embedded in the continuum at an energy close to the

[17] H. Feshbach, Ann. Phys. (N.Y.) **5**, 357 (1958); **19**, 287 (1962).
[18] W. M. MacDonald, Nucl. Phys. **54**, 393 (1964); **56**, 636 (1964).
[19] H. A. Weidenmüller, Nucl. Phys. **75**, 189 (1965).
[20] H. A. Weidenmüller and K. Dietrich, Nucl. Phys. **83**, 332 (1966).
[21] L. I. Garside and W. M. MacDonald, Phys. Rev. **138**, B582 (1965).
[22] H. A. Weidenmüller, Nucl. Phys. **A99**, 269 (1967); **A99**, 289 (1967).

energy of the isobaric analog resonance. Its coupling to the various continua gives rise to the isobaric analog resonance in the corresponding channels. Throughout the present investigation we will use the $g_{9/2}$ analog resonance in ^{209}Bi as an example to illustrate the formal developments. Numerical results are also presented for this case.

In the next section we discuss our choice of H_0 and some properties of its eigenstates. The sets of bound and continuum configurations, on which the diagonalization of the residual interaction is considered, are also specified in this section. The shell-model description of analog resonances is formulated in Sec. III. In Sec. IV we present numerical results obtained by diagonalizing the residual interaction on the bound neutron–neutron-hole–proton configurations in ^{209}Bi. The analog spin and isospin properties of the eigenstates are also discussed. The coupling of the isobaric analog state $|\Sigma\rangle$ to the various proton continua is treated in Sec. V. Isospin properties of the continuum wave functions are also discussed, and the scattering matrix elements are calculated. In Sec. VI the effects arising from the numerous $T_<$ states are considered, and the expressions for the energy-averaged scattering matrix elements are presented. Details of this calculation are given in Appendix A. We find that approximations used in Ref. 22, to treat the $T_<$ states, can be improved upon. Section VII is devoted to the discussion of the numerical results obtained in the calculations on the $g_{9/2}$ isobaric analog resonance in ^{209}Bi. The results are also compared with the experimental data of Richard *et al.*[23] The relevant formulas are given in Appendix B.

II. CHOICE OF INDEPENDENT PARTICLE HAMILTONIAN H_0

One simple choice for H_0 would be the interactions of the last nucleon or nucleon hole with the closed shells of 82 neutrons and protons represented by a one-body nuclear potential, which then would be the same for neutrons and protons. In accounting for the low-lying states in ^{209}Pb or ^{207}Pb, one would then need to consider the interactions of the last neutron or neutron hole with all the neutrons occupying the orbits from $N=82$ to 126. Similarly, for a description of low-lying states in ^{209}Bi or ^{207}Tl, it would be necessary to consider the interaction of the excess neutrons with the last proton or proton hole. The interaction of the last neutron (neutron hole) with the neutrons occupying the orbits between $N=82$ and 126 involves exchange terms which are absent in the interaction of the last proton (proton hole) with the excess neutrons. Thus, with this choice of H_0 the matrix elements of residual interactions for neutrons and protons are quite different. Indeed, this is the origin of the well-known symmetry term in the nuclear optical potential.

These considerations show that it will be desirable to choose an independent-particle Hamiltonian which provides an adequate description of the single-neutron states in ^{209}Pb as well as single-neutron–hole states in ^{207}Pb. Similarly, it should provide a description of the single-proton and single-proton–hole states in ^{209}Bi, and ^{207}Tl, respectively. If one searches for a one-body Saxon-Woods potential that provides the best description of the low-lying states in ^{209}Bi and ^{207}Tl, and a similar potential for states in ^{209}Pb and ^{207}Pb, one finds that the effective proton potential is about 15 MeV deeper than the neutron potential.

It is, however, possible to obtain a good description of the low-lying states in each of these four nuclei as single-nucleon or single-hole states. The second choice of H_0 is well suited to our description. With this choice, the residual interaction is *only* the interaction between particles and holes defined relative to ^{208}Pb. The effective two-body residual interaction corresponding to our choice of H_0 must be consistent with the difference between neutron and proton potentials employed in the definition of H_0. This consistency problem has been discussed by Pinkston.[24] In the following we will see that it leads to a constraint on the effective two-body residual interaction.

We now turn to the effective one-body potential for continuum eigenstates of ^{209}Bi with one proton in continuum. The empirically known optical potential that best describes the elastic scattering of protons from ^{208}Pb is complex and energy-dependent. The energy dependence and imaginary part of the optical potential are expected to arise naturally if one diagonalizes the residual interaction on the continuum eigenstates of H_0 and complicated bound eigenstates of H_0 lying in the vicinity of the excitation energy of the compound system. Empirically, one finds that the elastic scattering of protons from ^{208}Pb at energies between 14 and 19 MeV is well described by an optical potential whose real part has the same geometry as the bound-state potentials discussed above and depth given by

$$V_p = 66.3 - 0.4E_p, \tag{1}$$

where depth of the proton potential V_p and the proton energy E_p are expressed in MeV. Extrapolation of this well depth to small values of the proton energy E_p gives excellent agreement with the potential chosen for the proton bound states.

We choose the single-particle potentials for protons and neutrons to be different to accommodate the interaction of the last nucleon with the excess neutrons. This enables us to describe the low-lying states in ^{209}Pb, ^{207}Pb, ^{209}Bi, and ^{207}Tl as eigenstates of H_0. The real part of the optical potential that best describes

[23] P. Richard, W. G. Weitkamp, W. Wharton, H. Wieman, and P. von Brentano, Phys. Letters **26B**, 8 (1968).

[24] W. T. Pinkston, Nucl. Phys. **53**, 643 (1964).

the proton scattering is in very good agreement with the potential chosen to describe the low-lying bound states in ^{209}Bi and ^{207}Tl. Since we will not carry out the diagonalization of the residual interaction with respect to the continuum, our last-mentioned choice of proton potential seems to be very desirable. The parameters of the Saxon-Woods potentials employed are listed in Table I.

Our choice of H_0 has yet another merit in that the continuum eigenstates of H_0 with one proton in the continuum do not display single-particle resonances in a large energy region around the energy of the isobaric analog resonance. This is very important because close to the energy of a sharp single-particle resonance the amplitude of the continuum wave function becomes large in the nuclear interior. As a result, the continuum-continuum interaction is enhanced, and

TABLE I. Parameters of the Saxon-Woods potentials used to calculate the wave functions of neutrons and protons in bound states. The potential for the continuum eigenstates of proton has depth given by Eq. (1) and the same geometry as the bound-state potential.

	V_0 (MeV)	r_0 (F)	a (F)	$V_{s.o.}$ (MeV)
Neutrons	51	1.19	0.75	5.8
Protons	66	1.19	0.75	5.8

it may no longer be permissible to ignore it. It is covenient to define

$$I_\lambda(E)=\int_0^R [\psi_{\lambda E}(r)]^2 r^2 dr, \qquad (2)$$

where

$$\langle \psi_{\lambda E} \mid \psi_{\lambda E'} \rangle = \delta(E-E'),$$

and R is of the order of the nuclear radius. The quantity defined by Eq. (2) is a measure of the square of the amplitude of continuum wave function $\psi_{\lambda E}$ over the nucleus. In Figs. 1 and 2, $I(E)$ is plotted for two partial waves of interest for our choice of H_0 and for an independent-particle Hamiltonian obtained by equating the single-particle potentials for neutrons and protons.[22] We find similar qualitative behavior for other partial waves. Continuum eigenstates of the independent-particle Hamiltonian defined in the spirit of Ref. 22 display well-pronounced single-particle resonances in contrast to our choice. Technique discussed by Weidenmüller[22] for handling these single-particle resonances are useful only if they are sufficiently sharp, which holds only for low energies and high angular momenta.

Before concluding this section we mention that the Lane model[25] has been discussed and extended[26,27] in

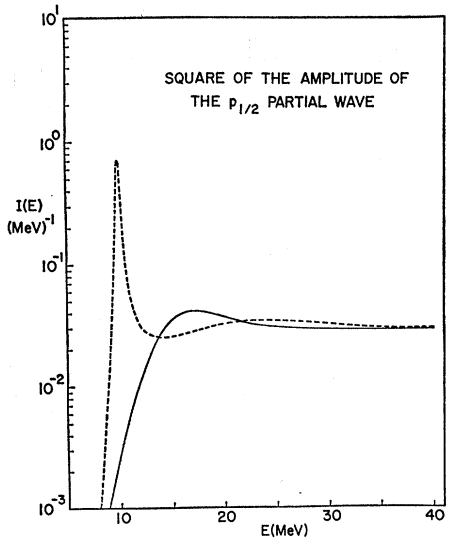

FIG. 1. Square of the amplitude of the $p_{1/2}$ continuum wave function, integrated over the nuclear volume. The ordinate is a measure of the continuum-continuum interaction involving two continuum wave functions, with the proton in the $p_{1/2}$ partial wave in each case. The dotted curve is calculated for an H_0 with $V_p=V_n$. The solid line corresponds to our choice of potentials.

the framework of the shell-model theory of reactions. The peculiar role of the residual interaction in splitting the proton single-particle resonance and *pushing away* a fraction $2T_0/(2T_0+1)$ of its strength is particularly transparent in these references. It is also clear, however, that the choice of H_0 implied in these references can be improved by including in H_0 all the

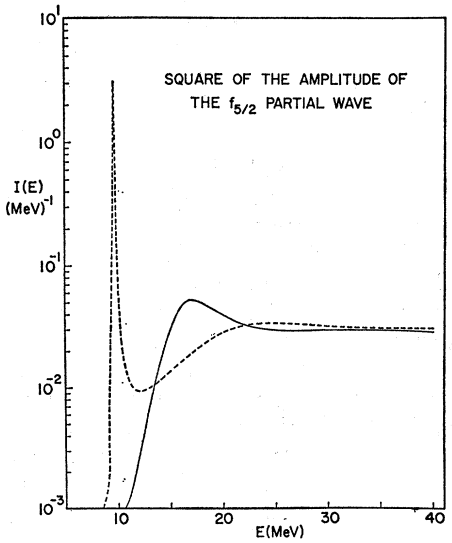

FIG. 2. Square of the amplitude of the $f_{5/2}$ continuum wave function, integrated over the nuclear volume. In this case the single-particle resonance displayed by the continuum wave function of H_0 with $V_p=V_n$ is much sharper than in the $p_{1/2}$ case. Also, for this partial wave, our choice of potentials considerably reduces the continuum-continuum interaction.

[25] A. M. Lane, Nucl. Phys. **35**, 676 (1962).
[26] C. Mahaux and H. A. Weidenmüller, Nucl. Phys. **A94**, 1 (1967).
[27] C. Mahaux, Z. Physik **196**, 240 (1966).

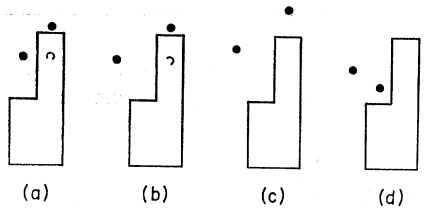

FIG. 3. Schematic representation of the 2-particle–1-hole bound and continuum eigenstates of H_0.

diagonal parts of the residual interaction, so that the residual interaction V consists entirely of the coupling between the (pC) and (nA) channels. This is, in effect, the approach adopted in Ref. 15. Recently Mekjian and MacDonald[28] and Tamura[29] have published theories of isobaric analog resonances which are based on a choice of H_0 similar to the one adopted here. Tamura critically discussed the various theories of isobaric analog resonances in considerable detail.

III. SHELL-MODEL DESCRIPTION OF ANALOG RESONANCES

The choice of one-body potentials made in the last section defines our independent-particle Hamiltonian H_0. We consider the following bound configurations $\{\phi_i\}$ that are eigenstates of H_0; a neutron in the $2g_{9/2}$ orbit together with a neutron hole in one of the excess neutron orbits and a proton in the corresponding proton orbit. The proton and the neutron-hole are coupled to zero total angular momentum, and we have a properly antisymmetrized two-particle, one-hole state. There is one such two-particle, one-hole state corresponding to each excess neutron orbit occupied in ^{208}Pb. In addition to these bound states, we consider the $g_{9/2}$ single-proton state in ^{209}Bi. This state is unbound by about 3.5 MeV. Being far below the Coulomb barrier and having an orbital angular momentum of 4, it gives rise to an extremely narrow single-particle resonance with an estimated width of less than *one-tenth of an electron volt*. In the following we treat this state ϕ_0 in exactly the same way as the true bound states $\{\phi_i\}$, ignoring the fact that it is unbound. Thus ϕ_0 is assumed to be the bound single-particle $2g_{9/2}$ proton state depicted in Fig. 3(a). We also introduce the set of continuum configurations $\chi_{0\epsilon}, \chi_{1\epsilon}, \cdots, \chi_{n\epsilon}$. Each of these is obtained from the corresponding bound configuration by replacing the bound single-proton state by a continuum solution with the same total angular momentum. The energy of the proton in continuum is denoted by ϵ. A typical continuum configuration of this type may be represented as shown in Fig. 3(b). It will be convenient to introduce the following notation for these 2p-1h wave functions:

$$\chi_{0\epsilon} = |\, J_0^*(\pi);\ J_0 M_0\rangle, \tag{3}$$

$$\chi_{i\epsilon} = |\, [J_i^*(\pi)\bar{J}_i(\nu)]_0 J_0(\nu);\ J_0 M_0\rangle. \tag{4}$$

The first one denotes a particle in the proton orbit 0, whereas the second one denotes a particle in the proton orbit i, a hole in the neutron orbit i coupled to a total angular momentum 0 and a particle in the neutron orbit 0. The asterisk is to remind us that a continuum state of that angular momentum is implied. The extremely narrow single-particle resonance displayed by the $g_{9/2}$ proton-continuum eigenstates is now to be excluded from $\chi_{0\epsilon}$, since it has already been included among the bound states as ϕ_0. The exclusion of this resonance from the $g_{9/2}$ proton-continuum states is straightforward, since it occurs far below the Coulomb barrier and is extremely sharp. This may be compared to the treatment of single-particle resonances by Garside and MacDonald.[21] Configurations similar to $\{\chi_{i\epsilon}\}$ have been used by a number of authors in discussing isobaric analog resonances; they are mentioned here for comparison. For the following discussion it is necessary to consider a larger set of continuum configurations. We introduce a set of 2-particle–1-hole configurations with the proton in a continuum state, with the energy ϵ, and with a definite state of total angular momentum; a neutron hole in one of the excess neutron orbits; and a neutron in one of the shell-model orbits beyond $3p_{1/2}$. The angular momentum of the proton is *not* necessarily the same as that of the neutron hole in this larger set. The angular momenta of neutron and the neutron hole are coupled to form the core spin I, which is coupled to the angular momentum of the proton in the continuum, to give the total angular momentum of the 2-particle–1-hole state. We denote these states by $\psi_{\beta\epsilon}$. Here β is an index specifying the set of quantum numbers of the core and the proton.

$$\psi_{\beta\epsilon} = |\, J_i^*(\pi)[\bar{J}_k(\nu)J_n(\nu)]_I;\ J_0 M_0\rangle. \tag{5}$$

A typical configuration of this type is shown in Fig. 3(c). Similarly, we include in $\{\psi_{\beta\epsilon}\}$ those configurations that involve a proton–proton-hole excitation of the core. One such configuration is depicted in Fig. 3(d).

$$\psi_{\beta\epsilon} = |\, J_i^*(\pi)[\bar{J}_p(\pi)J_q(\pi)]_I\ J_0 M_0\rangle. \tag{6}$$

We consider a total number of N such configurations $(\beta = 1, \cdots, N)$. It is clear that those functions of the set $\{\psi_{\beta\epsilon}\}$ that involve a neutron in the $g_{9/2}$ orbit and a neutron hole in one of the excess neutron orbits, together with a proton in the same angular-momentum state as the neutron hole, differ only in angular-momentum coupling from the functions of the set $\{\chi_{i\epsilon}\}$.

The Hamiltonian function of our system can now

[28] A. Mekjian and W. M. MacDonald, Nucl. Phys. **A121**, 385 (1968).
[29] T. Tamura, University of Texas technical report (unpublished); and Phys. Rev. (to be published).

be written

$$H=H_0+V, \tag{7}$$

where H_0 is the independent-particle Hamiltonian discussed in the last section. The configurations $\{\phi_i\}$, $\{\chi_{i\epsilon}\}$, and $\{\psi_{\beta\epsilon}\}$ are all eigenstates of H_0. We seek an expansion of the wave function of our system in terms of the configurations $\{\phi_i\}$, $\{\chi_{i\epsilon}\}$, and $\{\psi_{\beta\epsilon}\}$.

$$|\Psi\rangle\equiv\sum_i b_i|\phi_i\rangle+\sum_\beta\int d\epsilon a_\beta(\epsilon)|\psi_{\beta\epsilon}\rangle. \tag{8}$$

Putting this expansion into the Schrödinger equation, we get a system of coupled equations for the coefficients b_i and $a_\beta(\epsilon)$:

$$(E_i-E)b_i+\sum_j\langle\phi_i|V|\phi_i\rangle b_j+\sum_{\beta'}\int d\epsilon'\langle\phi_i|V|\psi_{\beta'\epsilon'}\rangle a_{\beta'}(\epsilon')=0, \tag{9}$$

$$\sum_j\langle\psi_{\beta\epsilon}|V|\phi_j\rangle b_j+(E_\beta+\epsilon-E)a_\beta(\epsilon)+\sum_{\beta'}\int d\epsilon'\langle\psi_{\beta\epsilon}|V|\psi_{\beta'\epsilon'}\rangle a_{\beta'}(\epsilon')=0. \tag{10}$$

The set of eigenstates $\{\psi_{\beta\epsilon}\}$ of H_0 that involve a proton in the continuum are not well suited to satisfy the boundary conditions of the scattering process being considered. Thus, for large values of the proton coordinate, the functions $\{\psi_{\beta\epsilon}\}$ describe the motion of a proton and a core configuration of 208 nucleons, which is in general not an eigenstate of ^{208}Pb. This is because the residual interaction has not been diagonalized on the particle-hole excitations of the ^{208}Pb core.[30] A change of basis functions $\{\psi_{\beta\epsilon}\}$ is required to accomplish this diagonalization. We observe that the matrix elements of the residual interaction between continuum eigenstates of the H_0 may be written

$$\langle\psi_{\beta\epsilon}|V|\psi_{\beta'\epsilon'}\rangle=\delta(\epsilon-\epsilon')\langle\beta|V_{\rm ph}|\beta'\rangle+\langle\psi_{\beta\epsilon}|V_d|\psi_{\beta'\epsilon'}\rangle. \tag{11}$$

The states $|\beta\rangle$ are eigenstates of H_0 corresponding to bound-particle–hole excitations of ^{208}Pb. The second term on the right-hand side involves transitions of the proton in continuum or its exchange with the bound proton depicted in Fig. 3(d), whereas the first term corresponds to the proton in continuum remaining in the same state. Returning to Eq. (10), we get

$$\sum_j\langle\psi_{\beta\epsilon}|V|\phi_j\rangle b_j+(E_\beta+\epsilon-E)a_\beta(\epsilon)+\sum_{\beta'}\langle\beta|V_{\rm ph}|\beta'\rangle a_{\beta'}(\epsilon)+\sum_{\beta'}\int d\epsilon'\langle\psi_{\beta\epsilon}|V_d|\psi_{\beta'\epsilon'}\rangle a_{\beta'}(\epsilon')=0. \tag{12}$$

[30] C. Bloch, in *Many-Body Description of Nuclear Structure and Reactions*, edited by C. Bloch (Academic Press Inc., New York, 1967).

We introduce continuum functions $\{\tilde\psi_{\lambda\epsilon}\}$ that are obtained through an orthogonal transformation over the set $\{\psi_{\beta\epsilon}\}$ and write

$$\psi_{\beta\epsilon}=\sum_\lambda\tilde\psi_{\lambda\epsilon}C_{\beta\lambda}, \tag{13}$$

which implies

$$a_\beta(\epsilon)=\sum_\lambda\tilde a_\lambda(\epsilon)C_{\beta\lambda}. \tag{14}$$

The coefficients $\tilde a_\lambda(\epsilon)$ are required to satisfy the equation

$$(E_\beta-E_\lambda)C_{\beta\lambda}+\sum_{\beta'}\langle\beta|V_{\rm ph}|\beta'\rangle C_{\beta'\lambda}=0. \tag{15}$$

In terms of the new basis for the continuum we get

$$(E_i-E)b_i+\sum_j\langle\phi_i|V|\phi_j\rangle b_j+\sum_{\lambda'}\int d\epsilon'\langle\phi_i|V|\tilde\psi_{\lambda'\epsilon'}\rangle\tilde a_{\lambda'}(\epsilon')=0, \tag{16}$$

$$\sum_j\langle\tilde\psi_{\lambda\epsilon}|V|\phi_j\rangle b_j+(E_\lambda+\epsilon-E)\tilde a_\lambda(\epsilon)+\sum_{\lambda'}\int d\epsilon'\langle\tilde\psi_{\lambda\epsilon}|V_d|\tilde\psi_{\lambda'\epsilon'}\rangle\tilde a_{\lambda'}(\epsilon')=0. \tag{17}$$

We observe that if we make another change of basis such that the Hamiltonian H_0 is diagonalized on the new basis $\{\tilde\phi_\mu\}$ for the bound configurations, then

$$(E_i-E_\mu)d_{i\mu}+\sum_j\langle\phi_i|V|\phi_j\rangle d_{j\mu}=0, \tag{18}$$

where

$$\tilde\phi_\mu=\sum_i d_{i\mu}\phi_i, \tag{19}$$

with $d_{i\mu}$, similar to the $C_{\beta\lambda}$, making up an orthogonal matrix. In terms of the sets $\{\tilde\phi_\mu\}$ and $\{\tilde\psi_{\lambda\epsilon}\}$, we finally obtain

$$(E_\mu-E)\tilde b_\mu+\sum_{\lambda'}\int d\epsilon'\langle\tilde\phi_\mu|V|\tilde\psi_{\lambda'\epsilon'}\rangle\tilde a_{\lambda'}(\epsilon')=0, \tag{20}$$

$$\sum_\mu\langle\tilde\psi_{\lambda\epsilon}|V|\tilde\phi_\mu\rangle\tilde b_\mu+(E_\lambda+\epsilon-E)\tilde a_\lambda(\epsilon)+\sum_{\lambda'}\int d\epsilon'\langle\tilde\psi_{\lambda\epsilon}|V_d|\tilde\psi_{\lambda'\epsilon'}\rangle\tilde a_{\lambda'}(\epsilon')=0. \tag{21}$$

The isobaric analog of the $g_{9/2}$ ground state of ^{209}Pb is observed at a proton energy of approximately 15 MeV. At this energy the cross sections for direct inelastic scattering are quite small in general. We conclude from this that the matrix elements of the interaction V_d between different continua are small in general. The direct inelastic scattering to the 3^- state at 2.6 MeV is, however, quite appreciable. This is due to the collective nature of that state. In the present analysis we wish to study the inelastic decay of the analog resonance into those channels in which the direct inelastic scattering is very small. If one now

TABLE II. The eigenvalues E_i and the expansion coefficients $d_{\mu i}$ of the eigenfunctions of Eq. (18) in terms of the bound eigenstates ϕ_i depicted in Fig. 3(a). The function ϕ_0 is simply a proton in the "bound" $g_{9/2}$ state in ^{209}Bi (see Sec. III). The function denoted by ϕ_1 has a neutron in the $2g_{9/2}$ state and a neutron hole and a proton in the *corresponding* $3p_{1/2}$ states. Similarly the function ϕ_2 has a neutron in the $2g_{9/2}$ state and a neutron hole and proton in the corresponding $2f_{5/2}$ states and so on. Finally, ϕ_6 has a proton and a neutron hole in the corresponding $1h_{9/2}$ states.

E_i	d_{0i}	d_{1i}	d_{2i}	d_{3i}	d_{4i}	d_{5i}	d_{6i}
15.030	+0.1262	+0.2077	+0.3712	+0.3059	+0.5290	+0.4213	+0.5023
6.567	+0.0508	+0.3708	+0.2061	+0.6174	−0.4446	+0.2385	−0.4262
4.568	−0.1232	+0.2194	−0.5124	+0.5505	+0.2174	−0.5323	+0.2012
3.058	+0.9297	−0.0035	+0.1216	−0.0017	−0.0086	−0.3469	−0.0210
3.297	−0.3115	−0.0776	+0.7221	+0.0668	+0.1442	−0.5769	−0.1318
3.744	−0.0593	+0.1114	+0.1446	−0.0495	−0.6656	−0.1355	+0.7067
3.547	−0.0373	+0.8676	−0.0008	−0.4640	+0.1068	−0.1038	−0.0915

neglects the coupling between different continua, realizes that with our choice of independent-particle Hamiltonian the continuum corresponding to the elastic channel has been diagonalized in the spirit of the optical model, and that each of the continua corresponding to the inelastic channels is also approximately diagonalized, then it seems reasonable to neglect the last term of Eq. (21). We are then left with

$$(E_\mu - E)\tilde{b}_\mu + \sum_{\lambda'} \int d\epsilon' \langle \tilde{\phi}_\mu \mid V \mid \tilde{\psi}_{\lambda'\epsilon'} \rangle \tilde{a}_{\lambda'}(\epsilon') = 0, \quad (22)$$

$$\sum_{\mu} \langle \tilde{\psi}_{\lambda\epsilon} \mid V \mid \tilde{\phi}_\mu \rangle \tilde{b}_\mu + (E_\lambda + \epsilon - E)\tilde{a}_\lambda(\epsilon) = 0. \quad (23)$$

IV. DIAGONALIZATION OF V ON THE BOUND CONFIGURATIONS $\{\phi_i\}$

To proceed further, we present the results of the diagonalization of an effective two-body residual interaction on the set of bound 2-particle–1-hole configurations. This amounts to the solution of the eigenvalue equation (18). As always, the particles and holes refer to the ^{208}Pb core. The zero-order energies are obtained from the experimentally observed separation energies of the corresponding low-lying single-particle states of ^{209}Pb, ^{207}Pb, and ^{209}Bi. (These zero-order energies are given in Table III.) The effective two-body interaction was chosen to be of the form

$$V(1,2) = \mathcal{U}(\mathbf{r}_1, \mathbf{r}_2) \times [V_{\mathrm{SE}} P_{\mathrm{SE}} + V_{\mathrm{TE}} P_{\mathrm{TE}} + V_{\mathrm{TO}} P_{\mathrm{TO}} + V_{\mathrm{SO}} P_{\mathrm{SO}}], \quad (24)$$

$$\mathcal{U}(\mathbf{r}_1, \mathbf{r}_2) = \exp(- \mid \mathbf{r}_1 - \mathbf{r}_2 \mid^2/\beta^2). \quad (25)$$

The projection operators P_{SE}, P_{TE}, P_{TO}, and P_{SO} have the usual meaning. Parameters of the two-body interaction chosen for this calculation were

$$V_{\mathrm{SE}} = -35.0 \text{ MeV}, \quad V_{\mathrm{TE}} = -52.5 \text{ MeV},$$

$$V_{\mathrm{TO}} = 5.0 \text{ MeV}, \quad V_{\mathrm{SO}} = 33.0 \text{ MeV},$$

and $\beta = 1.85$ F. These values were obtained as the result of an attempt to find an optimum description of the low-lying states of ^{208}Pb in terms of 1-particle–1-hole states. Indeed, these values are quite similar to those given by Carter, Pinkston, and True.[31] The matrix elements of this two-body interaction were calculated using wave functions of appropriate bound states of the single-particle potentials given above. Figure 4 shows the energies of the almost degenerate, unperturbed levels and the eigenvalues emerging from the shell-model calculation. Table II gives the expansion coefficients $d_{\mu i}$ of the eigenvectors of Eq. (18) in terms of the states ϕ_μ.

All reasonable choices of the two-body interaction display the same general features in their effect on the eigenvalue spectrum. One of the eigenvalues E_Σ is isolated and pushed up quite considerably, whereas the others are somewhat spread, but still lie close to the original unperturbed set of levels. Qualitatively

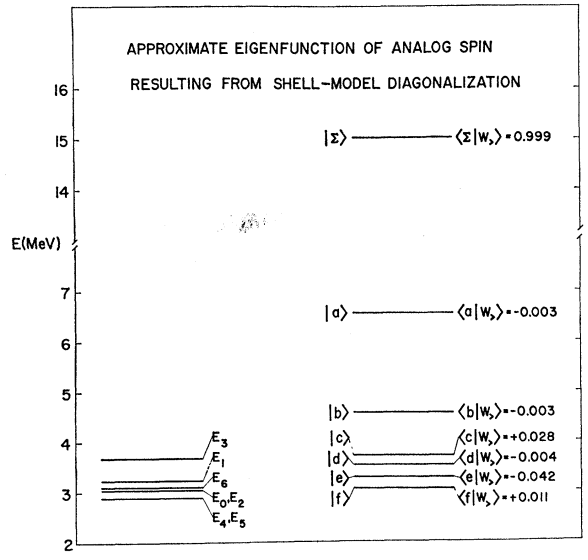

FIG. 4. Eigenenergies of the 2-particle–1-hole eigenstates of H_0 depicted in Fig. 3(a), and the result of the diagonalization of the residual two-body interaction on that set of states [Eq. (18)]. The new eigenenergies emerging from this shell-model calculation are shown together with the projections of the corresponding eigenstates on the analog spin eigenstate $\mid W_> \rangle$, defined by Eq. (26).

[31] J. C. Carter, W. T. Pinkston, and W. W. True, Phys. Rev. 120, 504 (1960).

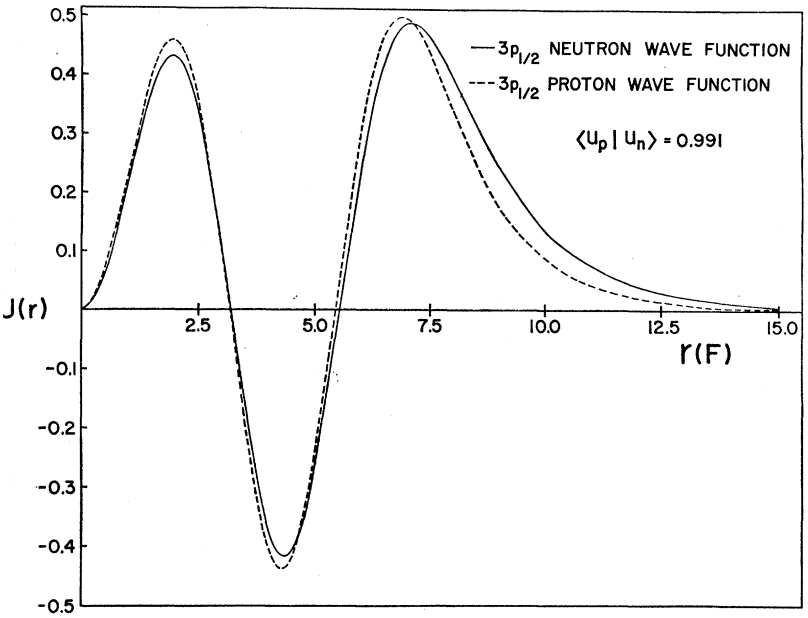

FIG. 5. Bound-state wave functions for the $3p_{1/2}$ state are shown both for a neutron and a proton. Although the functions appear to deviate somewhat from each other, their overlap is very close to unity.

this general behavior is expected and has been discussed by Pinkston.[24] We found that the singlet-odd component of the two-body interaction is not well determined by requiring that the above effective two-body interaction give an adequate description of the low-lying states of ^{208}Pb. We therefore have adjusted its strength so that the largest eigenvalue E_Σ lies approximately at the energy at which the $g_{9/2}$ isobaric analog resonance is observed in ^{209}Bi. It is hoped that the calculations[32] done with the effective interaction derived from the true two-body interaction would automatically predict the eigenstate $|\Sigma\rangle$ at an energy close to that of the isobaric analog resonance. Indeed, the constraint put on the effective two-body interaction, by requiring that the state $|\Sigma\rangle$ appear at a definite energy close to that of the observed isobaric analog resonance, is necessary for internal consistency of our description. This is clear if one recalls that the state $|\Sigma\rangle$ is expected to be separated from the ground state of ^{209}Pb essentially by an amount Q_{pn}, where Q_{pn} is the Q value for the "charge-exchange reaction" ^{209}Pb$(p, n)^{209}$Bi.[A]

We now consider briefly the nature of the state $|\Sigma\rangle$. It is convenient to define, for this purpose, the state $|W_>\rangle$ as

$$|W_>\rangle \equiv (N-Z+1)^{-1/2}(|\phi_0\rangle + \sum_i \hat{j}_i |\phi_i\rangle). \quad (26)$$

Here $N-Z$ is the neutron excess of ^{208}Pb and $\hat{j} \equiv (2j+1)^{1/2}$. This state is, by construction, an eigenstate of "analog spin."[33] In Fig. 4, the projections of this state on the eigenvectors of the shell-model calculations are given. The first row in Table II gives the expansion coefficients of this state in terms of the configurations $\{\phi_i\}$. The state $|\Sigma\rangle$ is rather close to being an eigenstate of analog spin. To investigate the isospin of the state $|\Sigma\rangle$ we define a state $|\xi\rangle$:

$$|\xi\rangle = (N-Z+1)^{-1/2}(|\zeta_0\rangle + \sum_i \hat{j}_i |\zeta_i\rangle), \quad (27)$$

where $|\zeta_0\rangle$ and $\{|\zeta_i\rangle\}$ are obtained from $|\phi_0\rangle$ and $\{|\phi_i\rangle\}$, respectively, by replacing the wave function of the extra proton by the wave function of a neutron in the corresponding orbit. Thus $|\xi\rangle$ may be considered as the isobaric analog of the excess neutron configuration in ^{209}Pb. The projection of $|\Sigma\rangle$ on $|\xi\rangle$ is found to be

$$\langle\Sigma|\xi\rangle = 0.995. \quad (28)$$

The large overlap between $|\Sigma\rangle$ and $|\xi\rangle$ is due to the large overlap between the corresponding neutron and proton single-particle wave functions. This is demonstrated for the $3p_{1/2}$ orbit in Fig. 5. It should be pointed out that $|\xi\rangle$ is not an eigenstate of the total isospin operator $\mathbf{T}^2$, since the wave functions for neutrons and protons occupying the single-particle states up to $N=82$ are not identical. The overlaps between the corresponding neutron and proton orbits for the single-particle states below the $1h_{9/2}$ are, however, larger than 99%. We remind ourselves that the radius parameter r_0 and the diffuseness have been chosen equal for neutrons and protons in the present case. The isospin purity of the state $|\Sigma\rangle$ would depend somewhat upon the choice of geometry; in particular, the optimum would be achieved if the radius param-

[32] T. T. S. Kuo and G. E. Brown, Nucl. Phys. **85**, 40 (1966).
[33] W. M. MacDonald, *Isobaric Spin in Nuclear Physics* (Academic Press Inc., New York, 1966).

eter r_0 for the potential proton were chosen slightly larger than that for the neutrons potential. We conclude that the state $|\Sigma\rangle$ is quite close to being an eigenstate of isospin; however, owing to uncertainties associated with the choice of single-particle potentials, it is not possible to investigate accurately the magnitude of the isospin admixture in $|\Sigma\rangle$.

V. DISCUSSION OF CONTINUUM SOLUTIONS AND S MATRIX

The state $|\Sigma\rangle$ is well isolated, so that in a limited energy region around the eigenvalue E_Σ we may neglect the coupling of other eigenvectors of Eq. (18) to the various continua.[34] Equations (22) and (23) then reduce to

$$(E_\Sigma-E)\tilde{b}_\Sigma+\sum_{\lambda'}\int d\epsilon'\langle\tilde{\phi}_\Sigma\,|\,V\,|\,\tilde{\psi}_{\lambda'\epsilon'}\rangle\tilde{a}_{\lambda'}(\epsilon')=0, \tag{29}$$

$$(E_\lambda+\epsilon-E)\tilde{a}_\lambda(\epsilon)+\langle\tilde{\psi}_{\lambda\epsilon}\,|\,V\,|\,\tilde{\phi}_\Sigma\rangle\tilde{b}_\Sigma=0, \qquad \lambda=1,\cdots,N. \tag{30}$$

In the terminology of the shell-model theory of reactions, these equations describe the coupling of a single bound configuration $|\Sigma\rangle$ to the continua $\{\tilde{\psi}_{\lambda\epsilon}\}$. The equations can be explicitly solved,[35] and one obtains

$$\Psi_E^{(\lambda)}=\tilde{b}_\Sigma^{(\lambda)}\times\left(\tilde{\phi}_\Sigma+\sum_\mu P\int d\epsilon\frac{V_{\Sigma\epsilon}^{(\mu)}\tilde{\psi}_{\mu\epsilon}}{E-E_\mu-\epsilon}-i\pi\sum_\mu V_\Sigma^{(\mu)}\tilde{\psi}_{\mu,E-E_\mu}+\frac{E-E_0+\frac{1}{2}i\Gamma}{V_\Sigma^{(\lambda)}}\tilde{\psi}_{\lambda,E-E_\lambda}\right). \tag{31}$$

The function $\tilde{\psi}_{\mu,E-E\mu}$ corresponds to the target nucleus being in one of its excited states (excitation energy E_μ) and the proton in continuum with the energy $E-E_\mu$. We have here and throughout used the abbreviations

$$V_{\Sigma\epsilon}^{(\lambda)}=\langle\tilde{\phi}_\Sigma\,|\,V\,|\,\tilde{\psi}_{\lambda\epsilon}\rangle, \qquad V_\Sigma^{(\lambda)}=\langle\tilde{\phi}_\Sigma\,|\,V\,|\,\tilde{\psi}_{\lambda,E-E_\lambda}\rangle. \tag{32}$$

Also note that

$$E_0=E_\Sigma+\Delta_\Sigma,$$

$$\Delta_\Sigma\equiv\sum_\lambda\Delta_\Sigma^{(\lambda)}=\sum_\lambda P\int\frac{V_{\Sigma\epsilon}^{(\lambda)}V_{\Sigma\epsilon}^{(\lambda)}}{E-E_\lambda-\epsilon}\,d\epsilon, \tag{33}$$

and

$$\Gamma=2\pi\sum_\lambda V_\Sigma^{(\lambda)}V_\Sigma^{(\lambda)}. \tag{34}$$

The above solution (31) satisfies the boundary condition that the only ingoing waves are in channel λ. There is one such solution for every continuum λ. The functions $\tilde{\psi}_{\lambda\epsilon}$ are normalized so that

$$\langle\tilde{\psi}_{\lambda\epsilon}\,|\,\tilde{\psi}_{\lambda'\epsilon'}\rangle=\delta_{\lambda\lambda'}\delta(\epsilon-\epsilon') \tag{35}$$

and[36]

$$\tilde{\psi}_{\lambda\epsilon}\longrightarrow(k/\pi\epsilon)^{1/2}\sin[kr-\tfrac{1}{2}\pi l+\delta_\lambda(\epsilon)]. \tag{36}$$

From the asymptotic form of $\Psi_E^{(\lambda)}$ one can now read off the S matrix:

$$\tilde{S}_{\lambda\mu}=\exp[i(\delta_\lambda+\delta_\mu)]\left(\delta_{\lambda\mu}-i\frac{(\Gamma_\Sigma^{(\lambda)})^{1/2}(\Gamma_\Sigma^{(\mu)})^{1/2}}{E-E_0+\frac{1}{2}i\Gamma}\right), \tag{37}$$

where

$$(\Gamma_\Sigma^{(\lambda)})^{1/2}=(2\pi)^{1/2}V_\Sigma^{(\lambda)}. \tag{38}$$

Notice that the partial-width amplitude $(\Gamma_\Sigma^{(\lambda)})^{1/2}$ is *defined* by Eq. (38) and is not necessarily positive. We have a Breit-Wigner resonance and a unitary S matrix. If we choose

$$\tilde{b}_\Sigma^{(\lambda)}=V_\Sigma^{(\lambda)}/(E-E_0+\tfrac{1}{2}i\Gamma), \tag{39}$$

then

$$\Psi_E^{(\lambda)}\longrightarrow(k_\lambda/\pi E_\lambda)^{1/2}\sin(k_\lambda r-\tfrac{1}{2}\pi l+\delta_\lambda)$$
$$-\tfrac{1}{2}\sum_\mu\left(\frac{k_\mu}{\pi E_\mu}\right)^{1/2}\frac{(\Gamma_\Sigma^{(\lambda)})^{1/2}(\Gamma_\Sigma^{(\mu)})^{1/2}}{E-E_0+\frac{1}{2}i\Gamma}\times\exp[i(k_\mu r-\tfrac{1}{2}\pi l_\lambda+\delta_\mu)], \tag{40}$$

and the ingoing parts of $\Psi_\Sigma^{(\lambda)}$ coincide with those of $\tilde{\psi}_{\lambda\epsilon}$ taken at $\epsilon=E-E_\lambda$.

We now wish to discuss the isospin of the solution $\Psi_E^{(\lambda)}$. It is convenient to start with the one-channel case, which can be obtained from Eq. (31) by specializing to one continuum $\tilde{\psi}_\epsilon$. Then

$$\Psi_E=\frac{V_\Sigma}{E-E_0+\frac{1}{2}i\Gamma}\left(\phi_\Sigma+P\int d\epsilon\frac{V_{\Sigma\epsilon}\tilde{\psi}_\epsilon}{E-\epsilon}+\frac{E-E_0}{V_\Sigma}\tilde{\psi}_E\right), \tag{41}$$

or

$$\Psi_E=(E-E_0+\tfrac{1}{2}i\Gamma)^{-1}\times\left[V_\Sigma\phi_\Sigma+P\int d\epsilon\frac{V_{\Sigma\epsilon}V_{\Sigma\epsilon}}{E-\epsilon}\left(\frac{\tilde{\psi}_\epsilon}{V_{\Sigma\epsilon}}\right)V_\Sigma+(E-E_0)\tilde{\psi}_E\right]. \tag{42}$$

To proceed further, we assume that the energy dependence of $(\tilde{\psi}_\epsilon/V_{\Sigma\epsilon})V_\Sigma$ may be ignored over the energy region which contributes significantly to the integral. Numerical calculations show that this is a good approximation if the proton coordinates in the continuum function $\tilde{\psi}_\epsilon$ are restricted to the nuclear dimensions. We obtain

$$\Psi_E=(E-E_0+\tfrac{1}{2}i\Gamma)^{-1}\{V_\Sigma\phi_\Sigma+\Delta_\Sigma\tilde{\psi}_E+(E-E_0)\tilde{\psi}_E\}, \tag{43}$$

[34] This is expected to be a very good approximation for a heavy nucleus like ^{209}Bi because although the states $|W_<\rangle$ are strongly coupled to a number of continua $\{\tilde{\psi}_{\lambda\epsilon}\}$, the effect of that coupling may be ignored in the neighborhood of the eigenvalue E_Σ which is about 9 MeV away from the eigenvalue of the closest $|W_<\rangle$ state (Fig. 4). In the case of lighter nuclei with small neutron excess this approximation may not be as good.

[35] U. Fano, Phys. Rev. **124**, 1866 (1961).

[36] Actually $\tilde{\psi}_{\lambda\epsilon}$ is a Slater determinant; Eq. (37) gives the asymptotic form of that function in the determinant that has nonvanishing amplitude asymptotically. For simplicity we imagine a screened Coulomb field.

or, since $E_0=E_\Sigma+\Delta_\Sigma$,

$$\Psi_E=(E-E_0+\tfrac{1}{2}i\Gamma)^{-1}\{V_\Sigma\phi_\Sigma+(E-E_\Sigma)\tilde{\psi}_E\}. \quad (44)$$

For energies in the neighborhood of E_Σ and over the nuclear region, the product $V_\Sigma\tilde{\psi}_E$ is only a few percent of ϕ_Σ, so that over an energy region of several times the width Γ the first term dominates. At the energy $E=E_\Sigma$ and over the nuclear region, the continuum solution becomes proportional to the bound configuration ϕ_Σ. In particular, it becomes as good an eigenstate of isospin as ϕ_Σ. This is the origin of the well-known asymmetry factor discussed originally by Robson.[37]

Making similar approximations in the multichannel case, we get

$$\Psi_E^{(\lambda)}=(E-E_0+\tfrac{1}{2}\Gamma)^{-1}\times\{V_\Sigma\tilde{\phi}_\Sigma+\sum_\mu(\Delta_\Sigma^{(\mu)}-\tfrac{1}{2}i\Gamma_\Sigma^{(\mu)})\times\tilde{\psi}_{\mu,E-E_\mu}+(E-E_0+\tfrac{1}{2}i\Gamma)\tilde{\psi}_{\lambda,E-E_\lambda}\}. \quad (45)$$

Clearly, the unique situation encountered in the single-channel case no longer prevails. The continuum solution now contains contributions from all open channels, and the amplitude in only one of these channels displays a zero. In the intermediate case, where the elastic channel dominates but other channels are also open, we expected to recover some features of the single-channel case.

To summarize, we have taken the coupling of the state $\tilde{\phi}_\Sigma$ to the various continua $\{\tilde{\psi}_{\lambda\epsilon}\}$ exactly into account. This coupling leads to the resonance behavior of each of the continua. The solution can be written explicitly in terms of the continua $\{\tilde{\psi}_{\lambda\epsilon}\}$, the state $\tilde{\phi}_\Sigma$, and the matrix elements of the residual interaction between $\tilde{\phi}_\Sigma$ and $\{\tilde{\psi}_{\lambda\epsilon}\}$. The strongly energy-dependent coefficients of this linear combination are given explicitly.

VI. $T_<$ STATES AND NEUTRON CONTINUA

In heavy nuclei, the isobaric analog resonances are observed at high excitation energies of the compound system. At these energies the density of compound-nuclear levels of $T_<$ isospin is rather high. These states $\{\Phi_k\}$, $k=1,\cdots,L$ by virtue of the high excitation energy, are expected to involve much more complicated shell-model configurations than those contained in the state $|\Sigma\rangle$. However, if the residual two-body interaction were diagonalized on a sufficiently large space of shell-model configurations, these complicated states would be expected to result from the calculation in a way similar to the state $|\Sigma\rangle$. Each of the states $\{\Phi_k\}$ generally will be coupled to each of the appropriate continuum states through the residual interaction. In addition to the functions defined by Eqs. (31) and (39), we now consider a number of functions $\{\Psi_E^{(\lambda)}\}$, $\lambda=N+1,\cdots,M$, each of which involves a neutron in the continuum, and the residual nucleus in one of the states that may be populated by a (p,n) reaction on the target nucleus under consideration. We have a total number M of functions, the first N of which describe a proton in continuum, and the rest of which describe a neutron in continuum. The states $\{\Phi_k\}$ will be coupled to the various continua through the residual interaction. This coupling would, for example, cause these states to decay into one of the neutron continua after they have been populated through one of the continua $\{\Psi_E^{(\lambda)}\}$, $\lambda=1,\cdots,N$.

In contrast to the states $\{\Phi_k\}$, the state $|\Sigma\rangle$ will be coupled only very weakly to the neutron continua. This is because ideally the wave functions that describe the neutron continua have isospin one unit less than the isospin of the state $|\Sigma\rangle$. A very weak coupling is expected, due to isospin admixtures in the low-lying states of the residual nucleus populated by the (p,n) reaction or to the isospin impurity of the state $|\Sigma\rangle$. In the following, we shall ignore the coupling of the state $|\Sigma\rangle$ to the neutron continua. The residual interaction is assumed already to be diagonalized on the neutron continua. In addition, we assume that the matrix elements of the residual interaction between different neutron continua are negligible. In addition, we assume that the matrix elements of the residual interaction between different neutron continua are negligible. This implies that the direct inelastic scattering of neutrons from the residual nucleus of the (p,n) reaction is negligible. In the framework of the above assumptions, it is now possible to solve the Lippman-Schwinger equation for the solution $\mathbf{\Psi}_E^{(\lambda)}$ of the total Hamiltonian on the space of functions $\{\Psi_E^{(\lambda)}\}$ and $\{\Phi_k\}$:

$$|\mathbf{\Psi}_E^{(\lambda)}\rangle=|\Psi_E^{(\lambda)}\rangle+\sum_{k,\mu}\int dE'(E^{(+)}-E')^{-1}|\Psi_{E'}^{(\mu)}\rangle\langle\Psi_{E'}^{(\mu)}|H|\Phi_k\rangle\langle\Phi_k|\mathbf{\Psi}_E^{(\lambda)}\rangle+\sum_{k,\mu}\int dE'(E-\epsilon_k)^{-1}|\Phi_k\rangle\langle\Phi_k|H|\Psi_{E'}^{(\mu)}\rangle\langle\Psi_{E'}^{(\mu)}|\mathbf{\Psi}_E^{(\lambda)}\rangle. \quad (46)$$

After a somewhat lengthy calculation given in Appendix A, one finally obtains the energy averages of the S-matrix elements if one invokes the statistical assumptions regarding the matrix elements involving the states $\{\Phi_k\}$. Indeed, this is just the approach of Ref. 22 as far as the effects arising from the $T_<$ states are concerned. We find,

[37] D. Robson, Phys. Rev. **137**, B535 (1965).

however, that the approximations made there can be improved upon, and one obtains results different from those reported by Weidenmüller.[22] For the energy average of the S-matrix elements, we find

$$S_{\lambda\mu}=\exp[i(\delta_\lambda+\delta_\mu)]\times\left(\delta_{\lambda\mu}\left|\frac{1-Y_\mu+2i(\Delta_\Sigma^{(\mu)}/\Gamma_\Sigma^{(\mu)})Y_\mu}{1+Y_\mu+2i(\Delta_\Sigma^{(\mu)}/\Gamma_\Sigma^{(\mu)})Y_\mu}\right|\exp[-i(\phi_\mu-\chi_\mu)]-i\exp[-i(\phi_\lambda+\phi_\mu)]\frac{(\tilde{\Gamma}_\Sigma^{(\lambda)})^{1/2}(\tilde{\Gamma}_\Sigma^{(\mu)})^{1/2}}{E-\mathcal{E}+\frac{1}{2}iG}\right),\quad(47)$$

where

$$(\tilde{\Gamma}_\Sigma^{(\lambda)})^{1/2}=(\Gamma_\Sigma^{(\lambda)})^{1/2}\mid a_{\lambda\lambda}\mid^{-1}\quad(48)$$

and

$$a_{\lambda\lambda}=1+Y_\lambda+2i(\Delta_\Sigma^{(\lambda)}/\Gamma_\Sigma^{(\lambda)})Y_\lambda=\mid 1+Y_\lambda+2i(\Delta_\Sigma^{(\lambda)}/\Gamma_\Sigma^{(\lambda)})Y_\lambda\mid\exp(i\phi_\lambda).\quad(49)$$

Also,

$$\mathcal{E}=E_0+\sum_\lambda\Delta_\Sigma^{(\lambda)}Y_\lambda\{2+Y_\lambda[1+4(\Delta_\Sigma^{(\lambda)}/\Gamma_\Sigma^{(\lambda)})^2]\}\mid a_{\lambda\lambda}\mid^{-2}\quad(50)$$

and

$$E_0=E_\Sigma+\sum_\lambda\Delta_\Sigma^{(\lambda)}.\quad(51)$$

Finally,

$$G=2\pi\langle V_\Sigma^2\rangle_{\rm av}/d+\sum_\lambda\tilde{\Gamma}_\Sigma^{(\lambda)}+\sum_\lambda\tilde{\Gamma}_\Sigma^{(\lambda)}Y_\lambda[1+4(\Delta_\Sigma^{(\lambda)}/\Gamma_\Sigma^{(\lambda)})^2]\quad(52)$$

and

$$\exp(i\chi_\lambda)=[1-Y_\lambda+2i(\Delta_\Sigma^{(\lambda)}/\Gamma_\Sigma^{(\lambda)})Y_\lambda]\times\mid 1-Y_\lambda+2i(\Delta_\Sigma^{(\lambda)}/\Gamma_\Sigma^{(\lambda)})Y_\lambda\mid^{-1}.\quad(53)$$

The quantities E_Σ, Δ_Σ, and $\Gamma_\Sigma^{(\lambda)}$ were defined in Sec. V. Finally, the quantities $2\pi\langle V_\Sigma^2\rangle_{\rm av}/d$ and Y_λ are defined in Eq. (A31). The most prominent difference between our results and those derived by Weidenmüller[22] is in the "effective partial-width amplitudes" $(\tilde{\Gamma}_\Sigma^{(\lambda)})^{1/2}$ and the corresponding quantities of his paper. We find that, due to the presence of $T<$ states, the background phase shifts δ_λ have not only acquired a complex part $i\eta_\lambda$ characterized by

$$\exp(-2\eta_\lambda)=\left|\frac{1-Y_\lambda+2i(\Delta_\Sigma^{(\lambda)}/\Gamma_\Sigma^{(\lambda)})Y_\lambda}{1+Y_\lambda+2i(\Delta_\Sigma^{(\lambda)}/\Gamma_\Sigma^{(\lambda)})Y_\lambda}\right|,\quad(54)$$

but that the *real* parts have also been modified. This result is comforting, since one does expect both the real and the imaginary parts of the optical-model phase shifts to be influenced by the coupling to the continuum of the complicated states $\{\Phi_k\}$.

The total width G may be written as the sum of the internal spreading width $2\pi\langle V_\Sigma^2\rangle_{\rm av}/d$ plus the summed partial widths $\tilde{\Gamma}_\Sigma^{(\lambda)}$ and the spreading width due to external mixing. Our expression for the external spreading width is again different from that derived in Ref. 22. In the limiting case $2\Delta_\Sigma^{(\lambda)}/\Gamma_\Sigma^{(\lambda)}\ll 1$ our expressions would agree with those of Ref. 22. However, in general we find that $2\Delta_\Sigma^{(\lambda)}/\Gamma_\Sigma^{(\lambda)}\sim 1$. The reason for the success of the expressions derived in Ref. 22 lies in the circumstance that Y_λ is typically of the order of 10% or less. This has the consequence that the factor multiplying the partial widths turns out to be close to unity. For heavy nuclei and isobaric analog resonances of low angular momenta, Y may be as large as 25%. In such cases the results of Ref. 22 would deviate quite significantly from ours.

VII. NUMERICAL RESULTS AND DISCUSSION

Differential cross sections for the inelastic scattering of protons to a number of final states in ^{208}Pb show a strong energy-dependence characteristic of a Breit-Wigner resonance.[9,38] At the $g_{9/2}$ resonance the ratio of the resonance scattering to the direct inelastic scattering background is as high as 40 for some states.[23] In many cases the cross sections also display symmetry about 90°. This indicates that in the description of inelastic scattering to *these* states it may be a good approximation to neglect the continuum-continuum interaction discussed at the end of Sec. V. To calculate the cross sections one needs to evaluate the partial-width amplitudes $\Gamma_{J_\lambda I J_0}{}^{1/2}$ defined by Eq. (B1). As explained in Appendix B, we shall restrict outselves to continuum functions involving only a neutron–neutron-hole excitation. In this case from (B1) and (B7) we obtain

$$\Gamma_{J_\beta I_\lambda J_0}{}^{1/2}=(\hat{I}_\lambda/\hat{J}_0)C_{\lambda\beta}\Gamma_{J_\beta J_0}{}^{1/2},\quad(55)$$

where we have defined

$$\Gamma_{J_\beta J_0}{}^{1/2}=(-1)^{J_\beta+I_\lambda+J_0}(1/\hat{J}_\beta)(2\pi)^{1/2}\sum_i d_{i\Sigma}\times{}_a\langle[J_\beta^*(\pi)\bar{J}_\beta(\nu)]_0\mid I_{\tilde{n}p}\mid[J_i(\pi)J_i(\nu)]_0\rangle_a.\quad(56)$$

Equation (55) gives the factorization of the partial-width amplitude into the coefficient $C_{\lambda\beta}$, which pertains to the structure of states of the target nucleus, and the quantity $\Gamma_{J_\beta J_0}{}^{1/2}$, which may itself be regarded as a decay-width amplitude. The latter is dependent only upon the structure of the state $\tilde{\phi}_\Sigma$. We shall refer to $\Gamma_{J_\beta J_0}$ as the partial width for pure configuration because it describes the decay of the state $\tilde{\phi}_\Sigma$ into a continuum which involves the core in a *pure* particle-hole configuration. Figure 6 shows these partial widths for the partial waves of interest as a function of the energy of the proton in continuum. These partial widths were calculated using the two-body force pa-

[38] W. R. Wharton, P. von Brentano, W. K. Dawson, and Patrick Richard, Phys. Rev. **176**, 1424 (1968).

rameters and eigenstates of H_0 discussed in Secs. III and IV, respectively. The details are given in Appendix B. Similarly, Fig. 7 shows the sum of the nuclear and Coulomb phase shifts for the partial waves of interest.

The coefficients $C_{\lambda\beta}$ were obtained from a Tamm-Dancoff calculation in which the two-body residual interaction of Sec. IV was diagonalized on the 1-particle–1-hole eigenstate of H_0. The shell-model orbits and the corresponding zero-order energies are given in Table III.

Matrix elements of the two-body interaction were evaluated using the single-particle wave functions calculated for the Saxon-Woods potentials for neutrons and protons given in Sec. II. Both the diagonal and off-diagonal matrix elements of the residual two-body Coulomb interaction were treated exactly. The eigenenergies given in Table III were obtained from Rost.[39] The eigenenergies of the $p_{1/2}$, $f_{5/2}$, and $p_{3/2}$ neutron orbits have been adjusted slightly to improve the agreement between the observed center of gravities of the $(g_{9/2}, p_{1/2}^{-1})$, $(g_{9/2}, f_{5/2}^{-1})$, and $(g_{9/2}, p_{3/2}^{-1})$ multiplets and the calculated center of gravities of these multiplets. States observed by Richard *et al.*[23] are compared with our calculation in Fig. 8. Finally, in Fig. 9 we compare our calculated cross sections with the experimental results obtained by Richard *et al.* The following resonance parameter[40] of the $g_{9/2}$ resonance in ^{209}Bi were employed in the calculation of the inelastic cross sections:

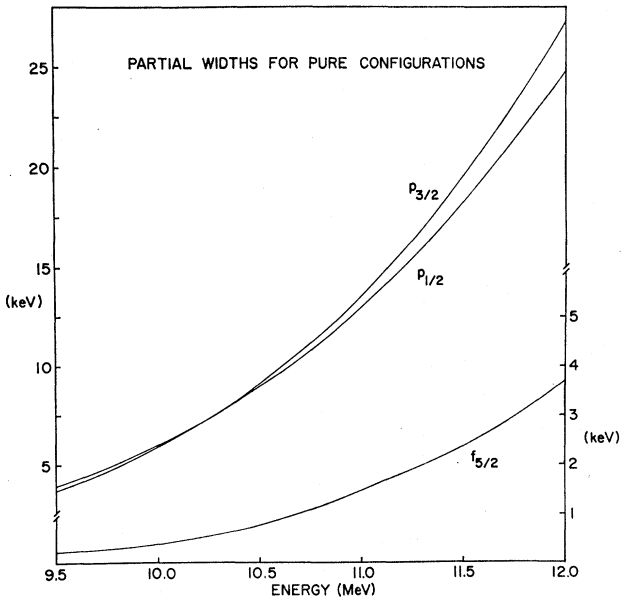

FIG. 6. Partial widths for pure configurations defined by Eq. (55) are shown for the three partial waves of interest as a function of the energy of the proton in continuum.

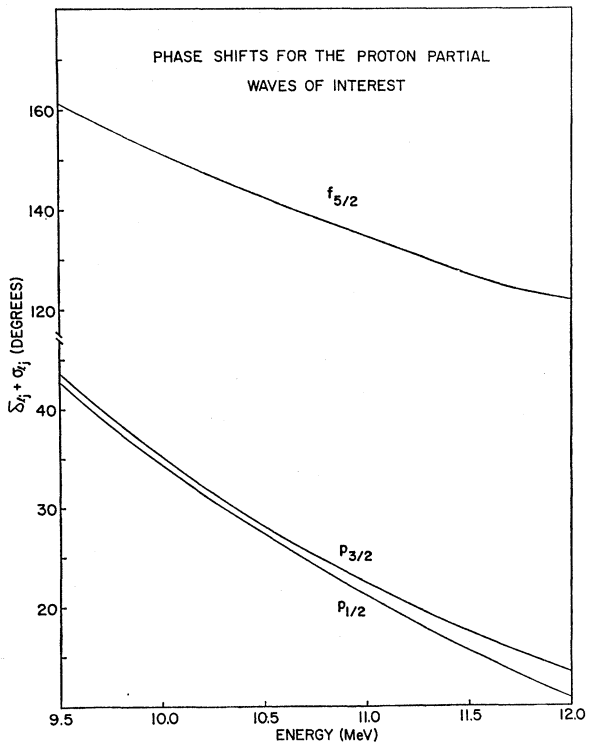

FIG. 7. The sum of the nuclear and Coulomb phase shifts $\delta_{lj}+\sigma_{lj}$ are shown as a function of the energy of the proton in the continuum.

resonance energy	14.98	MeV,
elastic proton width	25	keV,
total width	260	keV.

Comparison of the cross sections given in Ref. 23 with the corresponding values in Ref. 9 showed some discrepancies that are probably within the limits of experimental uncertainties of the experiments. The over-all agreement between the two experimental results is considerably improved if all the cross sections in Ref. 23 are multiplied by 0.8. The data shown in Fig. 9 are obtained in this way.

Comparisons of the calculated cross sections with experimental data revealed that the calculated angular distributions were much more sensitive to the nuclear structure of the excited states of ^{208}Pb (through the coefficients $C_{\lambda\beta}$) than to the details of the reaction mechanism. This is encouraging for studies of nuclear structure through analog resonances; however, the same circumstance makes it difficult to test the description of the reaction mechanism. Fortunately, there exist a number of states in ^{208}Pb that appear to be rather pure neutron–neutron-hole excitations. For such states the calculated inelastic scattering cross sections provide a test case for the description of the reaction mechanism. The 4^- state at 3.451 MeV, the 6^- state

[39] E. Rost, Phys. Letters **26B**, 184 (1968).
[40] S. Darmodjo, S. A. A. Zaidi, D. G. Martin, P. Dyer, and S. Ali (to be published).

TABLE III. Single-particle states and their eigenenergies used in the description of the low-lying states of ^{208}Pb as superpositions of particle-hole excitations.

Proton particle		Neutron hole		Neutron particle		Proton hole	
State	Eigenenergy (MeV)	State	Eigenenergy (MeV)	State	Eigenenergy (MeV)	State	Eigenenergy (MeV)
$3p_{1/2}$	−0.10	$3p_{1/2}$	7.22	$2g_{9/2}$	−3.940	$3s_{1/2}$	8.03
$3p_{3/2}$	−0.66	$2f_{5/2}$	7.86	$1i_{11/2}$	−3.170	$2d_{3/2}$	8.38
$2f_{5/2}$	−0.96	$3p_{3/2}$	8.10	$3d_{5/2}$	−2.380	$2d_{5/2}$	9.70
$2f_{7/2}$	−2.90	$2f_{7/2}$	9.71	$4s_{1/2}$	−1.910		
$1h_{9/2}$	−3.80	$1h_{9/2}$	10.84	$2g_{7/2}$	−1.470		
				$3d_{3/2}$	−1.420		

at 3.948 MeV, and the 6^- state at 4.463 MeV are predicted to be essentially pure $(g_{9/2}, p_{1/2}^{-1})$, $(g_{9/2}, f_{5/2}^{-1})$, and $(g_{9/2}, p_{3/2}^{-1})$ neutron–neutron-hole configurations, respectively. This result remains unchanged for all reasonable values of nuclear-force parameters and changes of the zero-order energies of these configurations. The agreement between theory and experiment for these states shows that our description of the reaction mechanism is basically correct.

The corrections arising from the "sea of $T_<$ states" surrounding the state $\tilde{\phi}_\Sigma$ were estimated to be small and were ignored. This is because the inelastically scattered protons have energies of the order of 11 MeV. The Y_λ occurring in Eqs. (47)–(54) are 10% or less. As a result, the partial widths are not modified by more than a few percent. In view of the simple shell-model description of the low-lying states of ^{208}Pb reported here, we do not expect the coefficients $C_{\lambda\beta}$ to provide an accurate description of the low-lying natural-parity states. However, the higher-lying states, particularly those of unnatural parity, are expected to be described correctly by our approach. Comparison of our calculations with experimental results allows us to assign spins and to identify dominant configurations of the excited states in ^{208}Pb. This knowledge will be useful in more sophisticated calculations for the excited states of ^{208}Pb.

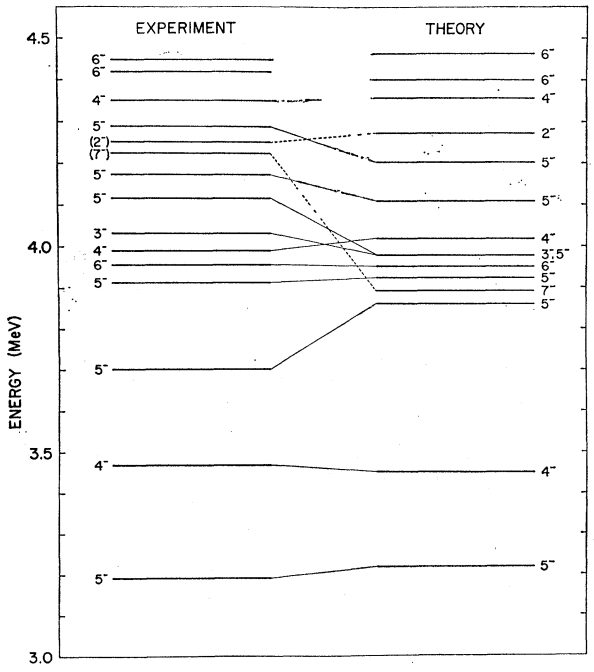

FIG. 8. Results of the Tamm-Dancoff calculation for the low-lying states of ^{208}Pb. Also shown are the states populated by the inelastic decay of the $g_{9/2}$ analog resonance in ^{209}Bi. Spin assignments of the observed levels are on the basis of the correspondence between observed and calculated cross sections shown in Fig. 9. The dotted lines for the 2^- and 7^- states are only meant to indicate the possible candidates for these spin values among the observed levels. These two assignments are uncertain.

We have shown that the microscopic description of analog resonances developed here predicts results in fair agreement with the experiment. The basic ideas underlying this description are simple, and the calculation can easily be performed for other nuclei. Indeed, our choice of independent-particle Hamiltonian H_0 which has the merit of greatly simplifying the residual interaction is a very natural one from the physical point of view. One aspect of this description that has generally been ignored in the literature is the coupling of the state $\tilde{\phi}_\Sigma$ to continua involving *proton–proton-hole* excitations of the target nucleus. In general, we expect the analog spin state $\tilde{\phi}_\Sigma$ to decay both into continua involving neutron–neutron-hole excitations of the target and continua involving proton–proton-hole excitations of the target. The relative importance of the two decay modes will be determined by the structure of the final state of the target nucleus. Thus the amplitude for the decay of an analog state $\tilde{\phi}_\Sigma$ into a low-lying collective state of the target nucleus may be a superposition of a number of amplitudes corresponding to each of the two decay modes. In this sense our microscopic description is capable of explaining the decay of analog resonances into low-lying collective states as well as simple particle-hole states of the target nucleus. It is clear, however, that for the description of collective states the simple particle-hole excitations considered here would not suffice. We planned to repeat these calculations in conjunction with improved shell-model calculations and to include approximately the effects arising from the continuum-continuum interaction neglected here.

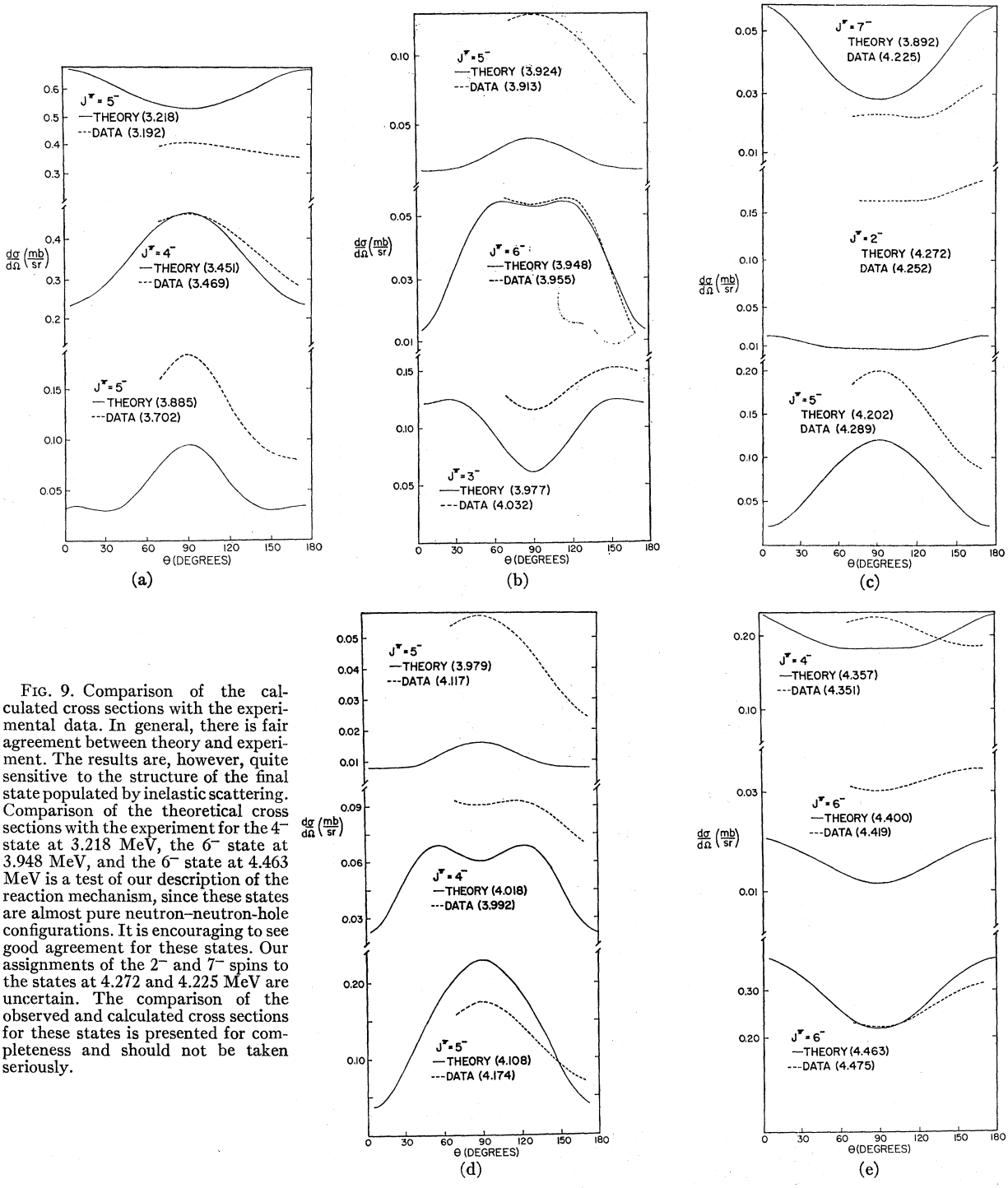

FIG. 9. Comparison of the calculated cross sections with the experimental data. In general, there is fair agreement between theory and experiment. The results are, however, quite sensitive to the structure of the final state populated by inelastic scattering. Comparison of the theoretical cross sections with the experiment for the 4^- state at 3.218 MeV, the 6^- state at 3.948 MeV, and the 6^- state at 4.463 MeV is a test of our description of the reaction mechanism, since these states are almost pure neutron–neutron-hole configurations. It is encouraging to see good agreement for these states. Our assignments of the 2^- and 7^- spins to the states at 4.272 and 4.225 MeV are uncertain. The comparison of the observed and calculated cross sections for these states is presented for completeness and should not be taken seriously.

ACKNOWLEDGMENTS

The authors acknowledge illuminating discussions with H. A. Weidemüller and T. Tamura. This investigation has also profited from several discussions with W. R. Coker, P. Richard, and K. P. Lieb. We are particularly thankful to W. R. Coker for help with computer programming and careful reading of the manuscript.

APPENDIX A: DETAILS OF CALCULATION LEADING TO AVERAGE S-MATRIX ELEMENTS

The Lippman-Schwinger (LS) equation (46) for the solution $\Psi_E^{(\lambda)}$ of the complete Hamiltonian H is

written in terms of the sets of continuum solutions $\{\Psi_E^{(\lambda)}\}$ and bound eigenstates $\{\Phi_k\}$. It is more convenient, however, to replace the set $\{\Psi_E^{(\lambda)}\}$ by a set of functions $\{F_E^{(\mu)}\}$ such that the matrix elements $\langle\Phi_k \mid H \mid F_E^{(\mu)}\rangle$ become real (the merits of this replacement will become evident in the following). This is accomplished by the unitary transformation

$$F_E^{(\lambda)}=\sum_\mu U_{\lambda\mu}\tilde{\Psi}_E^{(\mu)}, \tag{A1}$$

where

$$\tilde{\Psi}_E^{(\mu)}=\exp(i\delta_\mu)\Psi_E^{(\mu)}. \tag{A2}$$

The transformation matrix is

$$U_{\lambda\mu}=[1+\delta_{\lambda 1}(e^{-i\beta}-1)]O_{\lambda\mu}\exp(-i\delta_\mu), \tag{A3}$$

where

$$O_{1\mu}=(\Gamma_\Sigma^{(\mu)}/\Gamma)^{1/2};$$

$$e^{i\beta}=(E-E_0-\tfrac{1}{2}i\Gamma)/|E-E_0+\tfrac{1}{2}i\Gamma|, \qquad \Gamma=\Gamma_\Sigma. \tag{A4}$$

The rest of the matrix elements $O_{\lambda\mu}$ are arbitrary so long as O is an orthogonal matrix. Finally, δ_μ is the phase shift displayed by the function $\tilde{\psi}_\mu$ defined in Eq. (36). Similarly, we replace the function $\mathbf{\Psi}_E^{(\lambda)}$ by

$$\mathbf{F}_E^{(\lambda)}=\sum_\mu U_{\lambda\mu}\mathbf{\Psi}_E^{(\mu)}. \tag{A5}$$

The LS equation satisfied by $\mathbf{F}_E^{(\lambda)}$ expressed in terms of the sets $\{F_E^{(\lambda)}\}$ and $\{\Phi_k\}$ is identical in form to Eq. (46). It has the merit, however, that the matrix elements $\langle\Phi_k \mid H \mid F_E^{(\lambda)}\rangle$ occurring in it are real. This is easily solved[41] using techniques discussed in Ref. 20. The S-matrix elements can then be obtained by transforming back to the functions $\mathbf{\Psi}_E^{(\lambda)}$ and $\Psi_E^{(\lambda)}$. One obtains

$$S_{\lambda\mu}=\tilde{S}_{\lambda\mu}+2\pi i D^{(\lambda\mu)}/D. \tag{A6}$$

Here $\tilde{S}_{\lambda\mu}$ is given by (37) and $D=\det(D_{ik})$. The matrix D_{ik} is defined by

$$Di_k\equiv(E-E_i)\delta_{ik}-\sum_\lambda\int\frac{\langle\Phi_k \mid H \mid F_\epsilon^{(\lambda)}\rangle\langle F_\epsilon^{(\lambda)} \mid H \mid \Phi_i\rangle}{E^{(+)}-\epsilon}d\epsilon. \tag{A7}$$

The quantity $D^{(\lambda\mu)}$ is the determinant of a matrix obtained by adding a row and column to D_{ik}:

$$D_{\lambda\mu}=\det\begin{pmatrix} D_{ik} & \langle\Phi_k \mid H \mid \tilde{\Psi}_E^{(\mu)}\rangle \\ \langle\Phi_i \mid H \mid \tilde{\Psi}_E^{(\lambda)}\rangle & 0\end{pmatrix}. \tag{A8}$$

Using the explicit expression for the solutions $\Psi_E^{(\lambda)}$ given by Eqs. (31) and (39) and the definition (A1) of the functions $F_E^{(\lambda)}$, it is straightforward to calculate the matrix elements $\langle\Phi_i \mid H \mid F_E^{(\lambda)}\rangle$. One finds that

$$\langle\Phi_i \mid H \mid F_E^{(\lambda)}\rangle=(1-\delta_{\lambda 1})\sum_\mu O_{\lambda\mu}V_i^{(\mu)} +\delta_{\lambda 1}(\tfrac{1}{2}\Gamma/\pi)^{1/2}\,|E-E_0+\tfrac{1}{2}i\Gamma|^{-1} \times\left(V_{i\Sigma}+\sum_\sigma P\int d\epsilon\,\frac{V_{\Sigma\epsilon}^{(\sigma)}V_{i\epsilon}^{(\sigma)}}{E-\epsilon} +\frac{2\pi}{\Gamma}(E-E_0)\sum_\sigma V_i^{(\sigma)}V_\Sigma^{(\sigma)}\right). \tag{A9}$$

We have used the abbreviations

$$V_i^{(\mu)}\equiv\langle\Phi_i \mid H \mid \tilde{\psi}_{\mu,E-E_\mu}\rangle \quad\text{and}\quad V_{i\epsilon}^{(\sigma)}\equiv\langle\Phi_i \mid H \mid \tilde{\psi}_{\sigma\epsilon}\rangle, \tag{A10}$$

with similar expressions for $V_\Sigma^{(\mu)}$ and $V_{\Sigma\epsilon}^{(\mu)}$. Finally, we have written

$$V_{i\Sigma}\equiv\langle\Phi_i \mid H \mid \tilde{\phi}_\Sigma\rangle. \tag{A11}$$

The matrix elements $V_{i\Sigma}$ describe the mixing of the state $\tilde{\phi}_\Sigma$ into the numerous background states $\{\Phi_i\}$. It must be realized that the states $\{\Phi_i\}$ and the state $\tilde{\phi}_\Sigma$ are obtained by *separately* diagonalizing the residual interaction on suitably chosen sets of eigenstates of H_0.

In the spirit of approximations discussed in Sec. V, we can make good approximations to the principal-value integral occurring in Eq. (A9). That is,

$$P\int\frac{V_{\Sigma\epsilon}^{(\sigma)}V_{i\epsilon}^{(\sigma)}}{E-\epsilon}d\epsilon=P\int\frac{V_{\Sigma\epsilon}^{(\sigma)}V_{\Sigma\epsilon}^{(\sigma)}}{E-\epsilon}\frac{V_{i\epsilon}^{(\sigma)}}{V_{\Sigma\epsilon}^{(\sigma)}}d\epsilon \cong\frac{V_i^{(\sigma)}}{V_\Sigma^{(\sigma)}}P\int\frac{(V_{\Sigma\epsilon}^{(\sigma)})^2}{E-\epsilon}d\epsilon=\frac{V_i^{(\sigma)}}{V_\Sigma^{(\sigma)}}\Delta_\Sigma^{(\sigma)}. \tag{A12}$$

With the approximation for the principal-value integral one obtains

$$D_{ik}=(E-E_i)\delta_{ik}-\int\frac{f(\epsilon)d\epsilon}{E^{(+)}-\epsilon}, \tag{A13}$$

where we have written

$$f(\epsilon)=\sum_\mu V_{i\epsilon}^{(\mu)}V_{k\epsilon}^{(\mu)}-(2\pi/\Gamma)\sum_{\sigma\mu}V_{\Sigma\epsilon}^{(\mu)}V_{i\epsilon}^{(\mu)}V_{\Sigma\epsilon}^{(\sigma)}V_{k\epsilon}^{(\sigma)} +(\Gamma/2\pi)\,|\epsilon-E_0+\tfrac{1}{2}i\Gamma|^{-2}\{i\}\{k\} \tag{A14}$$

and introduced the abbreviation

$$\{i\}\equiv V_{i\Sigma}+\sum_\sigma\Delta_\Sigma^{(\sigma)}\frac{V_{i\epsilon}^{(\sigma)}}{V_{\Sigma\epsilon}^{(\sigma)}} +(2\pi/\Gamma)(\epsilon-E_0)\sum_\sigma V_{i\epsilon}^{(\sigma)}V_{\Sigma\epsilon}^{(\sigma)}. \tag{A15}$$

The integral involving the second and third terms in the definition of $f(\epsilon)$ can be evaluated by contour integration if one notices that the matrix elements $V_{i\epsilon}^{(\mu)}$ and $V_{\Sigma\epsilon}^{(\mu)}$ do not have singularities in a large energy region around the energy of interest $E\approx E_R$. This is evidenced by Figs. 1 and 2, in which the square of the continuum wave function integrated

[41] In Ref. 20 the S-matrix elements are derived formally for a given Lippman-Schwinger equation by assuming an expansion of the solution on a limited number of bound and continuum configurations. In deriving this result one assumes that a matrix similar to the one defined by Eq. (A7) can be diagonalized by a complex orthogonal transformation. This is always possible if D_{ik} is symmetric. This, on the other hand, requires that the matrix elements $\langle\Phi_i \mid H \mid F_\epsilon^{(\lambda)}\rangle$ and $\langle F_\epsilon^{(\lambda)} \mid H \mid \Phi_k\rangle$ occurring in (A7) be real.

over the nucleus is plotted as a function of energy. The continuum wave functions do not display any single-particle resonances, and we expect that $V_{i\epsilon}^{(\mu)}$ and $V_{\Sigma\epsilon}^{(\mu)}$ continued to complex energies would not have singularities in a sufficiently large part of the complex energy plane such that $|E-\epsilon| \gg \Gamma$ may be satisfied along a path in the ϵ plane that does not enclose singularities of $V_{i\epsilon}^{(\mu)}$ and $V_{\Sigma\epsilon}^{(\mu)}$. Then we have

$$\sum_\lambda \int \frac{\langle \Phi_i | H | F_\epsilon^{(\lambda)} \rangle \langle F_\epsilon^{(\lambda)} | H | \Phi_k \rangle}{E^{(+)}-\epsilon} d\epsilon = \sum_\mu \int \frac{V_{i\epsilon}^{(\mu)} V_{k\epsilon}^{(\mu)}}{E^{(+)}-\epsilon} d\epsilon + (E-\tilde{E})^{-1}\left(V_{i\Sigma}+\sum_\sigma \Omega^{(\sigma)} V_i^{(\sigma)} V_\Sigma^{(\sigma)}\right) \times \left(V_{k\Sigma}+\sum_\omega \Omega^{(\omega)} V_k^{(\omega)} V_\Sigma^{(\omega)}\right), \quad \text{(A16)}$$

where we have defined for brevity

$$\Omega^{(\sigma)} = -i\pi[1+2i(\Delta_\Sigma^{(\sigma)}/\Gamma_\Sigma^{(\sigma)})] \quad \text{and} \quad \tilde{E}=E_0-\tfrac{1}{2}i\Gamma. \quad \text{(A17)}$$

The first term on the right-hand side of (A16) may be written

$$\sum_\mu \int \frac{V_{i\epsilon}^{(\mu)} V_{k\epsilon}^{(\mu)}}{E^{(+)}-\epsilon} d\epsilon = \sum_\mu P \int \frac{V_{i\epsilon}^{(\mu)} V_{k\epsilon}^{(\mu)}}{E-\epsilon} d\epsilon - i\pi \sum_\mu V_i^{(\mu)} V_k^{(\mu)}. \quad \text{(A18)}$$

If one deletes the principal-value integral and retains only the imaginary part, then one obtains an expression for D_{ik} which finally leads to energy-average S-matrix elements similar in form to those reported in Ref. 22. Numerical calculations indicate, however, that the real part of the integral is generally as large as the imaginary part. It is thus not permissible to delete the first term and retain the second one. We approximate this principal-value integral in a way similar to that done above and obtain

$$\sum_\lambda \int \frac{\langle \Phi_i | H | F_\epsilon^{(\lambda)} \rangle \langle F_\epsilon^{(\lambda)} | H | \Phi_k \rangle}{E^{(+)}-\epsilon} d\epsilon = \sum_\mu \Omega^{(\mu)} V_i^{(\mu)} V_k^{(\mu)} + (E-\tilde{E})^{-1} \times \left(V_{i\Sigma}+\sum_\sigma V_i^{(\sigma)} V_\Sigma^{(\sigma)} \Omega^{(\sigma)}\right)\left(V_{k\Sigma}+\sum_\omega V_k^{(\omega)} V_\Sigma^{(\omega)} \Omega^{(\omega)}\right). \quad \text{(A19)}$$

Using the definitions

$$a_i^{(\mu)} = (\Omega^{(\mu)})^{1/2} V_i^{(\mu)}, \qquad \mu=1, \cdots, N, \; i=1, \cdots, L \quad \text{(A20)}$$

$$a_i^{0} = (E-\tilde{E})^{-1/2}\left(V_{i\Sigma}+\sum_\sigma V_i^{(\sigma)} V_\Sigma^{(\sigma)} \Omega^{(\sigma)}\right), \; i=1, \cdots, L \quad \text{(A21)}$$

we finally get

$$\sum_{\lambda=1}^{M} \frac{\langle \Phi_i | H | F_\epsilon^{(\lambda)} \rangle \langle F_\epsilon^{(\lambda)} | H | \Phi_k \rangle}{E^{(+)}-\epsilon} d\epsilon = \sum_{\mu=0}^{M} a_i^{(\mu)} a_k^{(\mu)}. \quad \text{(A22)}$$

In writing the above expression we have included the terms involving neutron continua ($\mu=N+1, \cdots, M$). These can be evaluated in the same manner as we treated the expression (A12). In the following we make statistical assumptions regarding the matrix elements involving the states $\{\Phi_i\}$. These assumptions lead to great simplifications in the expression for the energy-average S-matrix elements. For this purpose it is necessary to write the determinants D and $D^{\lambda\mu}$ in a different form,

$$D = \det\left[\delta_{ik}(E-E_i) - \sum_\lambda a_i^{(\lambda)} a_k^{(\lambda)}\right] = \prod_{i=1}^{L} (E-E_i) \det(M_{\lambda\mu}), \quad \lambda=0, \cdots, M, \; i=1, \cdots, L \quad \text{(A23)}$$

where

$$M_{\lambda\mu} = \delta_{\lambda\mu} - \sum_{i=1}^{L} \frac{a_i^{(\lambda)} a_i^{(\mu)}}{E-E_i}, \qquad \lambda, \mu=0, 1, \cdots, M, \; i=1, \cdots, L. \quad \text{(A24)}$$

The statistical assumptions are[22]

$$\langle V_i^{(\lambda)} V_i^{(\mu)} \rangle_{\text{av}} \cong \delta_{\lambda\mu} \langle (V^{(\lambda)})^2 \rangle_{\text{av}}, \quad \text{(A25)}$$

$$\langle V_i^{(\lambda)} V_{i\Sigma} \rangle_{\text{av}} \cong 0, \quad \text{(A26)}$$

$$\langle V_{i\Sigma} V_{i\Sigma} \rangle_{\text{av}} \cong \langle (V_\Sigma)^2 \rangle_{\text{av}}. \quad \text{(A27)}$$

The angular brackets imply average with respect to level index i. Performing the energy average, we obtain

$$\sum_{i=1}^{L} \frac{a_i^{(\mu)} a_i^{(\nu)}}{E-E_i} \cong -\frac{i}{\pi} \Omega^{(\mu)} Y_\mu \delta_{\mu\nu}, \qquad \mu, \nu=1, \cdots, N \quad \text{(A28)}$$

$$\sum_{i=1}^{L} \frac{a_i^{(\mu)} a_i^{(0)}}{E-E_i} \cong -\frac{i}{\pi} (E-\tilde{E})^{-1/2} (\Omega^{(\mu)})^{3/2} V_\Sigma^{(\mu)} Y_\mu, \qquad \mu=1, \cdots, N \quad \text{(A29)}$$

and

$$\sum_{i=1}^{L} \frac{a_i^{(0)} a_i^{(0)}}{E-E_i} \cong -\frac{i}{\pi} (E-\tilde{E})^{-1}\left[W+\sum_\sigma (V_\Sigma^{(\sigma)} \Omega^{(\sigma)})^2 Y_\sigma\right], \quad \text{(A30)}$$

where we have introduced the quantities

$$W = (\pi^2/d) \langle V_\Sigma^2 \rangle_{\text{av}} \quad \text{and} \quad Y_\mu = (\pi^2/d) \langle (V^{(\mu)})^2 \rangle_{\text{av}}. \quad \text{(A31)}$$

The average energy interval between the states Φ_i is denoted by d. The determinant $D^{\lambda\mu}$ involves the matrix elements

$$\langle \Phi_i | H | \tilde{\Psi}_E^{(\omega)} \rangle \equiv \tilde{Z}_i^{(\mu)} = \exp(i\delta_\mu)\left[(E-\tilde{E})^{-1/2} V_\Sigma^{(\mu)} a_i^{(0)} + V_i^{(\mu)}\right]. \quad \text{(A32)}$$

It is convenient to rewrite $D^{\lambda\mu}$ in a form similar to (A23):

$$D^{\lambda\mu}=\prod_i (E-E_i)\det(Q_{\lambda\mu}). \tag{A33}$$

$$Q_{\lambda\mu}=\begin{pmatrix} M_{\sigma\rho} & -\sum_i \tilde{Z}_i^{(\mu)}a_i^{(\rho)}/(E-E_i) \\ -\sum_i \tilde{Z}_i^{(\lambda)}a_i^{(\sigma)}/(E-E_i) & 0 \end{pmatrix}, \qquad \sigma,\rho,\lambda,\mu=1,\cdots,M,\ i=1,\cdots,L. \tag{A34}$$

One can again invoke the statistical assumptions (A25) and (A27) and obtain

$$\sum_i [\tilde{Z}_i^{(\mu)}a_i^{(0)}/(E-E_i)]\cong -(i/\pi)\exp(i\delta_\mu)(E-\tilde{E})^{-1/2}V_\Sigma^{(\mu)}\times\{(E-\tilde{E})^{-1}[W+\sum_\sigma (V_\Sigma^{(\sigma)}\Omega^{(\sigma)})^2 Y_\sigma]+\Omega^{(\mu)}Y_\mu\}, \tag{A35}$$

$$\sum_i [Z_i^{(\lambda)}Z_0^{(\mu)}/(E-E_i)]\cong -(i/\pi)\exp[i(\delta_\lambda+\delta_\mu)]\{Y_\mu\delta_{\lambda\mu}+(E-\tilde{E})^{-1}V_\Sigma^{(\mu)}V_\Sigma^{(\lambda)} \times(\Omega^{(\lambda)}Y_\lambda+\Omega^{(\mu)}Y_\mu)+(E-\tilde{E})^{-2}V_\Sigma^{(\lambda)}V_\Sigma^{(\mu)}[W+\sum_\sigma (V_\Sigma^{(\sigma)}\Omega^{(\sigma)})^2 Y_\sigma]\}, \tag{A36}$$

and

$$\sum_i [a_i^{(\lambda)}\tilde{Z}_i^{(\mu)}/(E-E_i)]\cong -(i/\pi)\exp(i\delta_\mu)Y_\lambda(\Omega^{(\lambda)})^{1/2}[\delta_{\lambda\mu}+(E-\tilde{E})^{-1}\Omega^{(\lambda)}V_\Sigma^{(\lambda)}V_\Sigma^{(\mu)}]. \tag{A37}$$

In terms of the following quantities the energy averages of the determinants D and $D^{\lambda\mu}$ take on a very simple form and are easily evaluated:

$$A_{\lambda\mu}=-\sum_{i=1}^{L}\frac{\tilde{Z}_i^{(\lambda)}\tilde{Z}_i^{(\mu)}}{E-E_i}, \qquad \lambda,\mu=1,2,\cdots,N \tag{A38}$$

$$A_{\alpha\lambda}=-\sum_{i=1}^{L}\frac{a_i^{(\alpha)}\tilde{Z}_i^{(\lambda)}}{E-E_i}, \qquad \lambda,\mathrm{d}=1,2,\cdots,N \tag{A39}$$

$$A_{\lambda 0}=-\sum_{i=1}^{L}\frac{\tilde{Z}_i^{(\lambda)}a_i^{(0)}}{E-E_i}, \qquad \lambda=1,2,\cdots,N \tag{A40}$$

$$a_{00}=1-\sum_{i=1}^{L}\frac{a_i^{(0)}a_i^{(0)}}{E-E_i},$$

$$a_{\alpha\beta}=\delta_{\alpha\beta}\sum_{i=1}\frac{a_i^{(\alpha)}a_i^{(\beta)}}{E-E_i}, \qquad \alpha,\beta=1,2,\cdots,N \tag{A41}$$

and

$$a_{\alpha 0}=-\sum_{i=1}^{L}\frac{a_i^{(\alpha)}a_i^{(0)}}{E-E_\alpha}, \qquad \alpha=1,2,\cdots,N. \tag{A42}$$

The energy-average S-matrix elements now become

$$\langle S_{\lambda\mu}\rangle_E=\tilde{S}_{\lambda\mu}+2\pi i\left(A_{\lambda\mu}-\sum_\alpha\frac{A_{\alpha\lambda}A_{\alpha\mu}}{a_{\alpha\alpha}}-\frac{(A_{\lambda 0}-\sum_\alpha a_{\alpha 0}A_{\alpha\lambda}/a_{\alpha\alpha})(A_{\mu 0}-\sum_\alpha a_{\alpha 0}A_{\alpha\mu}/a_{\alpha\alpha})}{a_{00}-\sum_\alpha a_{\alpha 0}a_{0\alpha}/a_{\alpha\alpha}}\right). \tag{A43}$$

Straightforward calculation now yields

$$S_{\lambda\mu}=\exp[i(\delta_\lambda+\delta_\mu)]\left((1-2Y_\mu a_{\mu\mu}^{-1})\delta_{\lambda\mu}-i\frac{(\Gamma_\Sigma^{(\lambda)})^{1/2}a_{\lambda\lambda}^{-1}(\Gamma_\Sigma^{(\mu)})^{1/2}a_{\mu\mu}^{-1}}{E-\tilde{E}+(i/\pi)[W+\sum_\omega (V_\Sigma^{(\omega)}\Omega^{(\omega)})^2 Y_\omega a_{\omega\omega}^{-1}]}\right), \tag{A44}$$

where

$$a_{\omega\omega}=1+Y_\omega+2i(\Delta_\Sigma^{(\omega)}/\Gamma_\Sigma^{(\omega)})Y_\omega. \tag{A45}$$

Finally, one can bring (A44) into the form given by Eq. (47)–(53) of Sec. VI.

APPENDIX B: CALCULATION OF PARTIAL WIDTHS AND CROSS SECTIONS

In this appendix we give in some detail the basic relationships between the partial-width amplitudes

$(\Gamma_\Sigma^{(\lambda)})^{1/2}$ and the matrix elements of two-body interactions. From Eq. (38) we have

$$\frac{(\Gamma_\Sigma^{(\lambda)})^{1/2}}{(2\pi)^{1/2}} \equiv \frac{\Gamma_{J_\beta I_\lambda J_0}^{1/2}}{(2\pi)^{1/2}} = \langle \tilde{\psi}_{\lambda,E-E_\lambda} \mid V \mid \tilde{\phi}_\Sigma \rangle. \quad \text{(B1)}$$

The index λ stands for quantum numbers needed to specify the continuum state $\tilde{\psi}_{\lambda,E-E_\lambda}$. This consists in the specification of the energy E_λ, the spin I_λ, and some additional quantum numbers pertaining to the residual nucleus. In addition, λ specifies the state of motion of the proton, which includes the energy and total angular momentum of the proton, $J_\beta(\pi)$. Finally, $\tilde{\psi}_{\lambda,E-E_\lambda}$ will be understood to imply the angular-momentum coupling

$$\mathbf{J}_\beta(\pi)+\mathbf{I}_\lambda=\mathbf{J}_0. \quad \text{(B2)}$$

The angular momenta are coupled in the order they appear in the equation, and $\mathbf{J}_0$ stands for the total angular momentum of the system. We now relate the matrix element in Eq. (B1) to matrix elements involving the shell-model configurations considered in Sec. III:

$$\langle \tilde{\psi}_{\lambda,E-E_\lambda} \mid V \mid \tilde{\phi}_\Sigma \rangle = \sum_i C_{\lambda\beta} d_{i\Sigma} \langle \psi_{\beta,E-E_\lambda} \mid V \mid \phi_i \rangle. \quad \text{(B3)}$$

We recall that $\{C_{\lambda\beta}\}$ are the coefficients of expansion of the final states of the residual nucleus in terms of 1-particle–1-hole excitations. The coefficients $\{d_{i\Sigma}\}$ give the amplitudes of the various 2-particle–1-hole configurations that make up the state $\tilde{\phi}_\Sigma$ [see Eq. (19)]. Numerical calculations show that for the $g_{9/2}$ isobaric analog resonance in ^{209}Bi the coefficients are very close to the following ones expected for an ideal analog state:

$$d_{i\Sigma} = (N-Z+1)^{-1/2}\hat{J}_i. \quad \text{(B4)}$$

Here and in the following we use the abbreviation $\hat{j}_i \equiv (2j_i+1)^{1/2}$. The numbers N and Z pertain to the target nucleus. However, it is not necessary to specialize to this ideal case. Making the angular momentum coupling more explicit, we write

$$\langle \psi_{\beta,E-E_\lambda} \mid V \mid \phi_i \rangle = {}_a\langle J_\beta^*(\pi)[\bar{J}_l(\nu)J_n(\nu)]_{I_\lambda} \times J_0 M_0 \mid V \mid [J_i(\pi)\bar{J}_i(\nu)]_0 J_0(\nu) J_0 M_0 \rangle_a. \quad \text{(B5)}$$

In this expression J_0M_0 stands for the spin of the isobaric analog resonance. The notation chosen is such that, for example, $J_n(\nu)$ denotes that the shell model state J_n is occupied by a neutron. A bar denotes that the state is occupied by a vacancy or hole. Finally, $J_\beta^*(\pi)$ implies that the particle is in the continuum with the total angular momentum J_β and a fixed energy $E-E_\lambda$. From now on we will delete the index λ and understand that the continuum functions are to be taken at the energy $E-E_\lambda$.

We are dealing with matrix elements of the residual interaction between 2-particle–1-hole configurations depicted in Fig. 3. The two-body interaction gives nonvanishing matrix elements between configurations making up the state $\tilde{\phi}_\Sigma$ and the 2-particle–1-hole configurations involving a proton in the continuum and the core in either a proton–proton-hole or neutron–neutron-hole configuration. We shall, however, restrict the discussion to those continuum functions that involve a neutron-particle–neutron-hole excitation of the target nucleus. This is because the simple shell model calculation for the bound states of ^{208}Pb considered in Sec. VII predicts small amplitudes for proton-particle–proton-hole excitation in the low-lying states of ^{208}Pb. Our description of the excited states of ^{208}Pb does not apply to low-lying collective levels like the 3^- state. The following three distinct contributions remain:

$$V = I_{\bar{n}p} + I_{\bar{n}n} + I_{np}. \quad \text{(B6)}$$

The first term is the neutron-hole–proton-particle interaction. The second gives the neutron-hole–neutron-particle interaction, and finally the third term is the neutron-particle–proton-particle interaction. We consider now the first contribution:

$${}_a\langle J_\beta^*(\pi)[\bar{J}_l(\nu)J_n(\nu)]_I J_0 M_0 \mid I_{\bar{n}p} \mid \times [J_i(\pi)\bar{J}_i(\nu)]_0 J_0(\nu) J_0 M_0 \rangle_a$$

If we restrict our discussion to spin-0 target nuclei, the nonvanishing contributions arise only for $J_n=J_0$ and $J_\beta=J_l$, in which case, by changing the coupling scheme on the left, we obtain

$$\begin{aligned} {}_a\langle J_\beta^*(\pi)[\bar{J}_l(\nu)J_n(\nu)]_I J_0 M_0 \mid I_{\bar{n}p} \mid [J_i(\pi)\bar{J}_i(\nu)]_0 \times J_0(\nu) J_0 M_0 \rangle_a &= (-1)^{I+J_\beta+J_0}(\hat{I}/\hat{J}_0\hat{J}_\beta) \\ \times {}_a\langle [J_\beta^*(\pi)\bar{J}_\beta(\nu)]_0 \mid I_{\bar{n}p} \mid [J_i(\pi)\bar{J}_i(\nu)]_0 \rangle_a \delta_{\beta l}\delta_{n0}. \end{aligned} \quad \text{(B7)}$$

The term involving the neutron–neutron-hole $I_{\bar{n}n}$ does not contribute if the bound single-proton wave functions are orthogonal to the wave functions describing the proton in continuum state. This is strictly true if both the continuum and bound-state functions are eigenstates of the same Hamiltonian. Similarly, for the contribution of the neutron-proton interaction we obtain

$$\begin{aligned} {}_a\langle J_\beta^*(\pi)[\bar{J}_l(\nu)J_n(\nu)]_I J_0 M_0 \mid I_{np} \mid [J_i(\pi)\bar{J}_i(\nu)]_0 J_0(\nu) J_0 M_0 \rangle_a &= (-)^{I+J_\beta+J_0} \sum_{I'} (\hat{I}'/\hat{J}_0\hat{J}_i)\hat{I}'\hat{I} \begin{Bmatrix} J_l & J_n & I \\ J_\beta & J_0 & I' \end{Bmatrix} \\ \times \langle J_\beta^*(\pi) J_n(\nu) I' \mid I_{np} \mid J_i(\pi) J_0(\nu) I' \rangle \delta_{li}. \end{aligned} \quad \text{(B8)}$$

The configuration on the right-hand side of the matrix element is in each case a typical component of the isobaric analog state $\tilde{\phi}_\Sigma$ and the one on the left-hand side is one of the continuum configurations $\{\psi_\beta\}$. It is interesting to note that the contribution considered in (B8) would lead to the decay of the isobaric analog state into a proton continuum such that the angular momentum of the neutron hole in the final nucleus

is *different* from that of the emitted proton. This possibility has generally been ignored in discussing the decay of isobaric analog resonances into particle-hole states of the residual nucleus, without much justification. Numerical calculations show, however, that this contribution is generally much smaller than the one given by (B7). The matrix element occurring in (B7) is easily evaluated. We have in general

$$\langle J_1^*(\pi)\bar{J}_2(\nu)JM \mid I_{\bar{n}p} \mid J_3(\pi)\bar{J}_4(\nu)JM\rangle$$
$$= -\sum_{J'}[J']\hat{J}_1\hat{J}_2\hat{J}_3\hat{J}_4\begin{Bmatrix} J_1 & J_2 & J \\ J_3 & J_4 & J' \end{Bmatrix} \times \sum_{\mathrm{LS}}[S][L]\begin{Bmatrix} s_3 & s_2 & S \\ l_3 & l_2 & L \\ J_3 & J_2 & J' \end{Bmatrix}\begin{Bmatrix} s_1 & s_4 & S \\ l_1 & l_4 & L \\ J_1 & J_4 & J' \end{Bmatrix} V(L,S), \quad \text{(B9)}$$

where $[J]\equiv 2J+1$ and

$$V(L,S) = (-1)^{l_1+l_2}\Big[(-1)^L[A-(-1)^S B]\sum_k \begin{Bmatrix} l_3 & l_2 & L \\ l_4 & l_1 & k \end{Bmatrix}(l_3 \| \mathbf{C}_k \| l_1)(l_2 \| \mathbf{C}_k \| l_4)R(l_3l_1 \mid l_2l_4)$$
$$+ [C-(-1)^S D]\sum_k \begin{Bmatrix} l_3 & l_2 & L \\ l_1 & l_4 & k \end{Bmatrix}(l_3 \| \mathbf{C}_k \| l_4)(l_2 \| \mathbf{C}_k \| l_1)R(l_3l_4 \mid l_2l_1)\Big]. \quad \text{(B10)}$$

We have defined the Slater integrals

$$R_k(l_3l_4 \mid l_2l_1) \equiv \iint u_{j_3}(r_1)u_{j_2}(r_2)f_k(r_1,r_2)u_{j_1}(r_2)u_{j_4}(r_1)r_1^2r_2^2dr_1dr_2 \quad \text{(B11)}$$

and used the multipole expansion

$$\mathcal{V}(|\mathbf{r}_1-\mathbf{r}_2|) = \sum_k f_k(r_1,r_2)\mathbf{C}_k(1)\cdot\mathbf{C}_k(2). \quad \text{(B12)}$$

The two-body interaction was taken as

$$V = \mathcal{V}(|\mathbf{r}_1-\mathbf{r}_2|)(A+BP^{(\sigma)}+CP^{(r)}+DP^{(\sigma)}P^{(r)}). \quad \text{(B13)}$$

The usual spin and space exchange operators are denoted by $P^{(\sigma)}$ and $P^{(r)}$. Radial wave functions occurring in (B11) are radial parts of the eigenstates of H_0, which includes spin-orbit interaction. Finally, we give the expression for the differential cross section derived from expression (37) for the S matrix:

$$(d\sigma/d\Omega)(0\to I) = (-1)^I(\lambda^2\Gamma_p/2\Gamma^2)(2J_0+1)(\cos^2\beta)$$
$$\times\sum_{L=0}^{2J_0-1}P_L(\cos\theta)\bar{Z}(l_0J_0l_0J_0;\tfrac{1}{2}L)$$
$$\times\sum_{J_1J_2}(-1)^{J_1+J_2}\cos(\delta_{J_1}-\delta_{J_2})\Gamma_{J_1IJ_0}{}^{1/2}\Gamma_{J_2IJ_0}{}^{1/2}$$
$$\times\bar{Z}(l_1J_1l_2J_2;\tfrac{1}{2}L)W(J_1J_0J_2J_0;IL). \quad \text{(B14)}$$

It is important to realize that the quantity $\Gamma_{J_1IJ_0}{}^{1/2}$ is defined by Eq. (B1) and is not necessarily positive. The elastic partial width and total width of the resonance are denoted by Γ_p and Γ, respectively. Also, spin and parity of the resonance are J_0 and $(-1)^{l_0}$, respectively. Finally, $\tan\beta=(E-E_R)/\frac{1}{2}\Gamma$ and E_R is the resonance energy.